High Constitutive Activity and a G-Protein-Independent High-Affinity State of the Human Histamine H_4-Receptor[†]

Erich H. Schneider,*[,‡] David Schnell,[‡] Dan Papa,[§] and Roland Seifert[||]

Department of Pharmacology and Toxicology, University of Regensburg, Universitätsstrasse 31, D-93040 Regensburg, Germany, Department of Pharmacology and Toxicology, University of Kansas, Lawrence, Kansas, and Institute of Pharmacology, Medical School of Hannover, Carl-Neuberg-Strasse 1, D-30625 Hannover, Germany

Received May 8, 2008; Revised Manuscript Received December 22, 2008

ABSTRACT: The human histamine H_4-receptor (hH_4R) is expressed in mast cells and eosinophils and mediates histamine (HA)-induced chemotaxis via G_i-proteins. For a detailed investigation of hH_4R/G_i-protein interaction, we coexpressed the hH_4R with $G\alpha_{i2}$ and $G\beta_1\gamma_2$ as well as an hH_4R-$G\alpha_{i2}$ fusion protein with $G\beta_1\gamma_2$ in Sf9 insect cells. The agonist radioligand [^{3}H]HA showed a K_D value of ~10 nM at hH_4R and hH_4R-$G\alpha_{i2}$. The high-affinity states of hH_4R and hH_4R-$G\alpha_{i2}$ were insensitive to guanosine 5′-[γ-thio]triphosphate (GTPγS). The affinity of [^{3}H]HA for hH_4R was retained in the absence of mammalian G_i-proteins. In steady-state GTPase- and [^{35}S]GTPγS-binding assays, hH_4R exhibited high constitutive activity and uncommon insensitivity to Na^+. Thioperamide (THIO) was only a partial inverse agonist. Addition of HA or THIO to baculovirus-infected ($hH_4R + G\alpha_{i2} + G\beta_1\gamma_2$) Sf9 cells increased the B_{max} in [^{3}H]HA binding, but not in immunoblots, suggesting conformational instability and ligand-induced stabilization of membrane-integrated hH_4R. No effect was observed on hH_4R-$G\alpha_{i2}$ expression, neither in [^{3}H]HA binding nor in immunoblot. However, the expression level of hH_4R-$G\alpha_{i2}$ was consistently higher compared to hH_4R, suggesting chaperone-like or stabilizing effects of $G\alpha_{i2}$ on hH_4R. In 37 °C stability assays, HA stabilized hH_4R, and THIO even restored misfolded [^{3}H]HA binding sites. Inhibition of hH_4R glycosylation by tunicamycin reduced the [^{3}H]HA binding B_{max} value. In conclusion, (i) hH_4R shows high constitutive activity and structural instability; (ii) hH_4R shows a G-protein-independent high-affinity state; (iii) hH_4R conformation is stabilized by agonists, inverse agonists and G-proteins; (iv) hH_4R glycosylation is essential for cell-surface expression of intact hH_4R.

The biogenic amine histamine (HA)[1] exerts numerous physiological effects by acting on four G-protein-coupled receptors (GPCRs). The H_1-receptor mediates, e.g., the increase of vascular permeability and NO production associated with inflammatory and allergic reactions (*1*). The H_2-receptor regulates gastric acid secretion and shows a positive inotropic effect on the heart (*1*). The presynaptic H_3-receptor negatively modulates neurotransmitter release in the CNS (*1*). The fourth HA receptor was first pharmacologically characterized on human eosinophils (*2*). It was cloned and identified as a GPCR with 390 amino acids by several research groups (*3*−*8*). The human H_4-receptor (hH_4R) shares 43% overall homology with the H_3-receptor (*4*).

The hH_4R is expressed, e.g., in spleen and bone marrow (*5, 8*). (−)-2-Cyano-1-methyl-3-{(2*R*,5*R*)-5-[1*H*-imidazol-4(5)-yl]tetrahydrofuran-2-yl}methylguanidine (OUP-16) (*9*), and 5-methylhistamine (*10*) were reported to be hH_4R-selective agonists. 1-[(5-Chloro-1*H*-indol-2-yl)carbonyl]-4-methyl-piperazine (JNJ-7777120) is the first selective hH_4R antagonist (*11*). The hH_4R mediates HA-induced chemotaxis of eosinophils (*12*), mast cells (*13*) and dendritic cells (*14*), indicating that it regulates inflammatory and immunological processes. This was confirmed by animal experiments, where JNJ-7777120 was effective in the treatment of pruritus (*15*), colitis (*16*) or allergic airway inflammation (*17*). hH_4R expression on the promyelocyte cell line HL-60 clone 15 is increased upon differentiation to eosinophils (*5*), which points to an additional role in promyelocyte differentiation.

Knowledge on the G-protein coupling selectivity of hH_4R is necessary for a better understanding of its physiological role and for the development of optimized functional test systems. Pertussis toxin (PTX) inhibits H_4R-mediated chemotaxis of mast cells (*13*) and the H_4R-induced cytoskeletal changes of eosinophils (*18*), indicating that the H_4R couples to G-proteins of the $G\alpha_i$ class. This was confirmed by the observation that histamine inhibits forskolin-stimulated cAMP synthesis in reporter gene assays (*3, 5, 7, 10*).

[†] This work was supported by the German Research Foundation (DFG, research training program GRK 766: "Medicinal Chemistry: Molecular Recognition−Ligand-Receptor-Interactions").

* To whom correspondence should be addressed: Telephone: +49-941-4786. Fax: +49-941-4772. E-mail: erich.schneider@chemie.uni-regensburg.de.

[‡] University of Regensburg.

[§] University of Kansas. Present address: Biopharmaceutical Analysis, Aptuit, Kansas City, MO.

[||] Medical School of Hannover.

[1] Abbreviations: hH_4R, human histamine H_4 receptor; HA, histamine; THIO, thioperamide; GPCR, G-protein-coupled receptor; FPR-26, formyl peptide receptor 26; GTPγS, guanosine 5′-[γ-thio]triphosphate; PTX, pertussis toxin; DHA, dihydroalprenolol; FMLF, *N*-formyl-L-methionyl-L-leucyl-L-phenylalanine (formyl peptide); α_2AR, α_2-adrenoceptor; β_2AR, β_2-adrenoceptor; CXCR4, chemokine receptor for stroma cell-derived factor-1, CB_1R, cannabinoid receptor 1; CAM, constitutively active mutant.

10.1021/bi802050d CCC: $40.75
Published on Web 01/23/2009

According to the two-state model of receptor activation (*19, 20*), GPCRs exist in an equilibrium of an active G-protein-coupling conformation (R*) and an uncoupled inactive state (R). R* promotes GDP/GTP exchange at the Gα subunit and shows a higher affinity for agonists than R. Thus, agonists activate the receptor by stabilizing an R* state. Neutral antagonists bind to R and R* states with the same affinity without altering the equilibrium. Some receptor molecules spontaneously adopt the R* state and promote G-protein signaling in the absence of agonists, which is referred to as constitutive or basal activity. Inverse agonists bind preferentially to the R state and reduce the basal activity. The hH_4R is constitutively active, and the hH_3R antagonist thioperamide (THIO) acts as an inverse agonist at the hH_4R (*4, 5, 10*).

The cellular test systems existing to date have several disadvantages, which hamper a detailed investigation of the H_4R on the molecular level. For example, for the preparation of eosinophils large volumes of blood are needed, since their concentration in human blood is low. When the hH_4R is expressed in mammalian cell lines, it has to be coexpressed with chimeric G-proteins, e.g. $G\alpha_{qi5}$ (*3*), or with the promiscuous G-protein $G\alpha_{15}$ (*7*), in order to obtain a calcium response. Many groups use reporter gene assays (*3, 5, 7, 10*). However, in these assays, a parameter very distal from the receptor activation event is determined, and the linearity of the signal transfer may be compromised by several amplification steps in the signal transduction cascade. This may, e.g., hamper the discrimination between partial and full agonists.

The Sf9 cell/baculovirus system is well suited for the high-level expression of recombinant GPCRs. For example, the $G\alpha_i$-coupled formyl peptide receptor (FPR-26), a classic chemoattractant receptor expressed in leukocytes, was functionally reconstituted in Sf9 cells by coexpression with $G\alpha_{i2}$ and $G\beta\gamma$ subunits (*21*). The preparation of GPCR-Gα fusion proteins ensures a 1:1 stoichiometry of receptor and G-protein and minimizes interactions with insect cell G-proteins. In this way, a quantitative analysis of FPR-26 coupling to $G\alpha_{i1}$, $G\alpha_{i2}$, and $G\alpha_{i3}$ was performed (*22*).

GPCR/G-protein coupling in Sf9 cell membranes can be investigated at a point very proximal to the ligand binding event by determination of steady-state GTPase activity or GDP/[^{35}S]GTPγS exchange. Since Sf9 cells lack endogenous constitutively active receptors (*21, 23*), the signaling background is very low, which facilitates the investigation of constitutive activity. The extent of ternary complex formation can be determined in agonist binding assays by comparing B_{max} and K_d values in the presence and the absence of GTP or GTPγS (*24*). In combination with the results from [^{35}S]GTPγS binding assays, such experiments provide valuable data for the development of receptor activation models.

Here, we report on the functional reconstitution of the H_4R in Sf9 cells for the detailed investigation of receptor activation and G-protein coupling.

EXPERIMENTAL PROCEDURES

Materials. The pcDNA 3.1 plasmid with the hH_4R sequence was obtained from the UMR cDNA Resource Center at the University of Missouri-Rolla (Rolla, MO). *Pfu* polymerase was obtained from Stratagene (La Jolla, CA). The DNA primers for PCR were synthesized by MWG Biotech (Ebersberg, Germany). Recombinant baculovirus encoding the unmodified versions of the $G\beta_1\gamma_2$ subunits was a kind gift of Dr. P. Gierschik (Department of Pharmacology and Toxicology, University of Ulm, Germany). Baculoviruses for $G\alpha_{i1}$, $G\alpha_{i2}$, and $G\alpha_{i3}$ were donated by Dr. A. G. Gilman (Department of Pharmacology, University of Southwestern Medical Center, Dallas, TX). Baculovirus encoding rat $G\alpha_o$ was generously provided by Dr. J. C. Garrison (University of Virginia, Charlottesville, VA). Purified rat $G\alpha_{i2}$ protein for immunoblotting was obtained from Dr. B. Nürnberg (Institute of Pharmacology, University of Tübingen, Germany). The antibodies selective for $G\alpha_{i1/2}$ and $G\alpha_o$ were purchased from Calbiochem; the M1 anti-FLAG antibody was obtained from Sigma (St. Louis, MO). The H_4R antagonist JNJ-7777120 was kindly provided by Dr. R. Thurmond (Department of Immunology, Johnson & Johnson Pharmaceutical R & D, San Diego, CA). A 10 mM stock solution of JNJ-7777120 was prepared in Me_2SO. The stock solutions (10 mM) and dilutions of all other H_4R agonists and antagonists described in this paper were prepared in distilled water. Tunicamycin was obtained from Sigma (St. Louis, MO). [^{3}H]HA (specific activity 18.1 Ci/mmol) was obtained from Perkin-Elmer (Boston, MA). [γ-^{32}P]GTP was prepared in our laboratory using GDP and [^{32}P] (orthophosphoric acid, 150 mCi/mL, obtained from Perkin-Elmer) according to a previously described enzymatic labeling procedure (*25*). All other reagents were of the highest purity available from standard suppliers. Radioactive samples were counted in a PerkinElmer Tricarb 2800TR liquid scintillation analyzer.

Construction of FLAG Epitope and Hexahistidine-Tagged hH_4R cDNA. In order to enhance membrane insertion of the hH_4R, a DNA sequence encoding the cleavable signal peptide from influenza hemagglutinin followed by the FLAG epitope, which can be recognized by the M1 antibody, was placed 5′ of the start codon of the hH_4R DNA. Moreover, a hexahistidine tag was added to the hH_4R C-terminus to allow future purification of the receptor and to enhance stability against proteolysis. These modifications were generated by sequential overlap-extension PCR using *Pfu* polymerase.

In PCR 1a, the DNA sequence of the signal peptide (S) and the FLAG epitope (F) was amplified. We used a plasmid containing the SF sequence as template, the sense pGEM primer (5′-GCT CAC TCA TTA GGC ACC-3′), which starts 5′ of the *Sac*I site of the pGEM-3Z plasmid and an antisense primer encoding a part of the SF sequence followed by the receptor start codon (5′-CAT GGC GTC ATC ATC GTC-3′). In PCR 1b, the cDNA of the hH_4R was amplified using pcDNA3.1-hH_4R as template with the sense primer HRH4-F (5′-GAC GAT GAT GAC GCC ATG CCA GAT ACT AAT AG-3′) and the antisense primer HRH4-RV (5′-GAT CCT CTA GAT TAG TGA TGG TGA TGA TGG TGA GAA GAT ACT GAC CG-3′). The HRH4-F primer anneals with the first 17 bp of the 5′-end of the hH_4R sequence and includes the last 15 bp of the SF-peptide in its 5′-extension. The HRH4-RV comprises the sequence encoding the last five C-terminal amino acids of the hH_4R, followed by the hexahistidine tag, the stop codon, and a final *Xba*I restriction site. In PCR2, the products of PCRs 1a and 1b were used as templates. The sense pGEM primer and the HRH4-RV primer were used to generate a fragment encoding a sequence containing the *Sac*I site followed by the signal sequence, the FLAG epitope, the hH_4R DNA, the hexahistidine tag, and an *Xba*I site. This fragment was digested with *Sac*I and

*Xba*I and directly cloned into a baculovirus expression vector pVL1392 containing the same restriction sites in its multiple cloning site.

Construction of the hH_4R-$G\alpha_{i2}$ Fusion Protein. The hexahistidine-tagged C-terminus of the hH_4R was fused to the N-terminus of $G\alpha_{i2}$ by overlap extension PCR using *Pfu* polymerase. The sense primer $s6HG\alpha_{i2}$ (5′-CAC CAT CAT CAC CAT CAC ATG GGC TGC ACC GTG AGC-3′) and the antisense primer $a6HG\alpha_{i2}$ (5′-GCT CAC GGT GCA GCC CAT GTG ATG GTG ATG ATG GTG-3′) were synthesized. Both primers encode the hexahistidine tag and 18 bp from the N-terminus of $G\alpha_{i2}$. In PCR 1a, the sequence between the primer s*Eco*RI-hH_4 (5′-GCC ATC ACA TCA TTC TTG GAA TTC GTG ATC CCA GTC-3′), which contains the *Eco*RI site of the hH_4R, and the $a6HG\alpha_{i2}$ fusion primer was amplified using the pGEM-3Z-SF-H_4R-His_6 plasmid as template. In PCR 1b, the $G\alpha_{i2}$ sequence between the $s6HG\alpha_{i2}$ fusion primer and the antisense primer a$G\alpha_{i2}$-*Xba*I (5′-GGT CGA CTC TAG AGG TCA GAA GAG GCC ACA GTC-3′) was amplified using the pGEM-3Z-SF-β_2AR-His_6-$G\alpha_{i2}$ plasmid as template. In PCR 2, the products of PCR 1a and 1b were used as templates together with the primers s*Eco*RI-hH_4 and a$G\alpha_{i2}$-*Xba*I. This resulted in a fragment encoding a part of the hH_4R beginning at the *Eco*RI site, followed by a hexahistidine tag and the $G\alpha_{i2}$ sequence with an *Xba*I site 3′ of the stop codon. This fragment was digested with *Eco*RI and *Xba*I and cloned into pGEM-3Z-SF-hH_4R-His_6 digested with the same enzymes to obtain the full-length fusion protein DNA sequence. PCR-generated DNA sequences were confirmed by sequencing (Entelechon, Regensburg, Germany). The fusion protein DNA was cloned into the baculovirus expression vector, pVL1392.

Generation of Recombinant Baculoviruses, Cell Culture, and Membrane Preparation. Sf9 cells were cultured in 250 or 500 mL disposable Erlenmeyer flasks at 28 °C under rotation at 150 rpm in SF 900 II medium (Invitrogen, Carlsbad, CA) supplemented with 5% (v/v) fetal calf serum (Biochrom, Berlin, Germany) and 0.1 mg/mL gentamicin (Cambrex Bio Science, Walkersville, MD). Cells were maintained at a density of $(0.5-6.0) \times 10^6$ cells/mL. Recombinant baculoviruses were generated in Sf9 cells using the BaculoGOLD transfection kit (BDPharmingen, San Diego, CA) according to the manufacturer's instructions. After initial transfection, high-titer virus stocks were generated by two sequential virus amplifications. The supernatant fluid from the second amplification was stored under light protection at 4 °C and used as routine virus stock for membrane preparations.

Infection of the cells with baculoviruses was performed as previously described (*26*). The virus stocks were combined as described in the Results section. Sf9 membranes were prepared as described (*27*), using 1 mM EDTA, 0.2 mM phenylmethylsulfonyl fluoride, 10 μg/mL benzamidine, and 10 μg/mL leupeptin as protease inhibitors. Membranes were suspended in binding buffer (12.5 mM $MgCl_2$, 1 mM EDTA, and 75 mM Tris/HCl, pH 7.4) and stored at −80 °C until use.

The preparation of membranes expressing unglycosylated hH_4R was performed essentially as previously described for FPR-26 (*28*). Tunicamycin (5 mg/mL in 10 mM NaOH) was added to the baculovirus-infected cell suspension to yield final concentrations of 10 μg/mL for tunicamycin and 20 μM for Na^+. Due to the buffering capacity of the culture medium, the pH value did not change significantly. The same volume of 10 mM NaOH solution without tunicamycin was added to a baculovirus-infected control cell culture. After 48 h, the membranes were prepared as described above.

To determine the effect of THIO and HA on the expression levels of hH_4R and hH_4R-$G\alpha_{i2}$, mini membrane preparations were performed as follows: For one preparation, 15×10^6 Sf9 cells were seeded in a 75 cm^2 culture flask (15 mL cell culture medium). THIO (100 μM) and HA (1 mM) solutions were added to the corresponding flasks to yield final concentrations of 1 and 10 μM for THIO and HA, respectively. The baculovirus suspensions were added to yield a final 1:100 dilution. Cells were incubated at 28 °C for 48 h. To compensate degradation, HA (10 μM) was readded after 24 h. After 48 h, cells were harvested by shaking the flask and centrifugation of the cell suspension at 4 °C and 1000 rpm. Cells were washed once with phosphate-buffered saline, and after centrifugation (4 °C, 1000 rpm), they were suspended in 0.5 mL of lysis buffer. The lysis buffer contained protease inhibitors and was prepared as described for the regular membrane preparations (*27*). The cells were homogenized by repeatedly (25×) drawing up the suspension using a 1 mL syringe with a 27 gauge needle. After a 10 min centrifugation at 13 000 rpm and 4 °C, the pellet was washed with 1 mL of lysis buffer and centrifuged again (4 °C, 13 000 rpm). Finally, the pellet was resuspended in 2 mL of binding buffer and frozen in 0.5 mL aliquots. The membrane was stored at −80 °C.

[^{3}H]HA Binding Experiments. Prior to the experiments, membranes were sedimented by a 10 min centrifugation at 4 °C and 13 000 rpm and resuspended in binding buffer (12.5 mM $MgCl_2$, 1 mM EDTA, and 75 mM Tris−HCl, pH 7.4). For determination of K_d and B_{max} values, Sf9 membranes (50−100 μg of protein per tube, depending on the specific expression level) were suspended in 250 or 500 μL of binding buffer supplemented with [^{3}H]HA (1−100 nM) and 0.2% (mass/vol) bovine serum albumin. Nonspecific binding was determined in the presence of 10 μM THIO. For competition binding experiments, 10 nM of [^{3}H]HA and five appropriate concentrations between 1 nM and 10 μM of the test compound were used. Incubations were performed for 60 min at 25 °C and shaken at 250 rpm. Bound radioligand was separated from free radioligand by filtration through GF/C filters pretreated with 0.3% (m/v) polyethyleneimine and washed three times with 2 mL of ice-cold binding buffer (4 °C). Filter-bound radioactivity was determined by liquid scintillation counting.

hH_4R Stability Assays. In the literature, stability assays were reported for purified β_2AR_{CAM} protein (*29*) or the α_{2a}AR expressed in CHO cell membranes (*30*). Using these protocols, we developed a modified procedure, which can be performed with hH_4R-expressing Sf9 cell membranes in 2 mL reaction vials. This allows the use of a cooled table-top centrifuge for 2 mL vials throughout the experiment. We used about 10-fold more membrane protein as in the α_{2a}AR protocol (*30*) in order to compensate for the loss of membrane caused by the slower centrifugation speed. The hH_4R stability assay was performed as outlined below.

Prior to the experiments, membranes were sedimented by a 10 min centrifugation at 4 °C and 13 000 rpm. Membranes were suspended in binding buffer (cf. [^{3}H]HA binding

section) + 0.4% (m/v) BSA to yield a final concentration of 8 μg/μL of membrane protein. To determine THIO-mediated hH_4R "refolding", 50 μL of the membrane suspension was mixed with 50 μL of BSA-free binding buffer to yield a final concentration of 0.2% (m/v) BSA and 4 μg/μL of membrane protein. This sample represented the conformationally intact control sample and was incubated in triplicate at 4 °C in parallel to the 37 °C samples throughout the assay. The remaining fraction of the membrane suspension was incubated for 45 min at 37 °C (inactivation step). Thereafter, 50 μL aliquots of this suspension were mixed with 50 μL of binding buffer without BSA (solvent sample) or with 50 μL of solutions of THIO (20 μM) or HA (20 μM) in binding buffer (without BSA), to yield a final concentration of 10 μM for THIO or HA and 0.2% (m/v) for BSA. The solvent, THIO, and HA samples were incubated in triplicate for additional 45 min at 37 °C.

Thereafter, all samples (conformationally intact sample at 4 °C, solvent, HA and THIO samples at 37 °C) were diluted 20-fold with 1.9 mL of ice-cold binding buffer (without BSA) and centrifuged immediately at 4 °C and 13 000 rpm for 10 min. Each membrane pellet was resuspended in 2 mL of ice-cold binding buffer (without BSA), and the suspension was centrifuged again for 10 min at 4 °C and 13 000 rpm. Finally, each pellet was suspended in 200 μL of ice-cold binding buffer. B_{max} of [^{3}H]HA was determined by adding 50 μL of these suspensions to reaction vials containing binding buffer, BSA and [^{3}H]HA to yield a final concentration of 0.2% (m/v) BSA and 100 nM [^{3}H]HA. From every third replicate, 50 μL was incubated in the presence of 10 μM of THIO (in addition to 0.2% (m/v) BSA and 100 nM [^{3}H]HA) to determine nonspecific binding. All binding samples were incubated for 60 min at room temperature and processed as described above for the [^{3}H]HA Binding Experiments. Since membrane protein gets lost during the washing steps, 20 μL from the residual volumes of all membrane suspension samples was used to determine the final protein concentration.

For stabilization assays without investigation of THIO-mediated receptor refolding, the solvent and HA (10 μM) and THIO (10 μM) samples were incubated for 120 min at 37 °C and the conformationally intact sample was incubated in parallel on ice. After 120 min, the samples were washed and prepared for binding assays as described above.

To determine the time course of receptor denaturation, a membrane suspension (1.8 μg/μL) in binding buffer (without BSA) was incubated for 180 min at 37 °C and mixed every 15−30 min to prevent sedimentation. After 0, 30, 70, 120 and 180 min of incubation, 50 μL aliquots (in triplicate) were added to reaction vials containing 25 μL of H_2O (or 25 μL of 100 μM THIO solution for nonspecific binding) and 150 μL of ice-cold binding buffer with 0.33% (m/v) BSA. The reaction vessels were placed on ice to stop the receptor inactivation. Finally, the [^{3}H]HA binding assay was started with all samples simultaneously by addition of 25 μL of 1 μM [^{3}H]HA to yield a final volume of 250 μL, containing 0.2% (m/v) BSA, 100 nM [^{3}H]HA, and 90 μg of membrane per sample. The binding assay was performed as described above for the [^{3}H]HA Binding Experiments.

GTPγS Binding Assays. Before the experiments, membranes were sedimented by a 10 min centrifugation at 4 °C and 13 000 rpm. Membranes were resuspended in binding buffer. GTPγS saturation binding studies were performed in binding buffer in the presence of 1 μM GDP, 100 mM NaCl, and 0.05% (w/v) bovine serum albumin (BSA). Every sample contained 0.8−2.5 nM [^{35}S]GTPγS mixed with varying concentrations of unlabeled GTPγS to yield the final ligand concentrations. The protein content of the samples was 5−20 μg of membrane protein per 250 or 500 μL. The respective ligands were added as 10-fold concentrated stock solutions. Incubations were performed for 240 min at 25 °C and shaken at 250 rpm. All samples were filtered simultaneously, using a Brandel Harvester.

For time course studies, the samples were mixed as described for the saturation binding assays, but with a [^{35}S]GTPγS concentration of 0.4 nM. A sample volume of 1700 μL with a membrane concentration of 0.03 μg/μL was used. All samples were started simultaneously, incubated at 25 °C, and shaken at 250 rpm. At different times, 175 μL aliquots containing 5.25 μg of membrane protein were removed from the total sample volume and filtered by a Millipore 1225 vacuum sampling manifold (Millipore, Bedford, MA). Nonspecific [^{35}S]GTPγS binding was determined in the presence of 10 μM GTPγS and was less than 0.4% of total binding. In saturation binding assays as well as in binding kinetics, bound [^{35}S]GTPγS was separated from free [^{35}S]GTPγS by filtration through GF/C filters, followed by three washes with 2 mL of binding buffer (4 °C). Filter-bound radioactivity was determined by liquid scintillation counting.

Steady-State GTPase Assay. Steady-state GTPase assays were essentially performed as previously described in ref (*26*) but with 5.0 mM $MgCl_2$, 1.2 mM creatine phosphate, and 1 μg of creatine kinase in the samples. If not indicated otherwise, each tube additionally contained 100 mM NaCl. The samples for the determination of Gα enzyme kinetics were prepared with a higher amount of [γ-^{32}P]GTP (0.4−0.5 μCi/tube). Unlabeled GTP was added in increasing concentrations from 0 to 1500 nM. Due to the displacement of [γ-^{32}P]GTP from the Gα subunit, the signal-to-noise ratio of the GTPase signal is reduced by unlabeled GTP. Therefore, unlabeled GTP was not used at concentrations higher than 1.5 μM.

SDS-PAGE and Immunoblot Analysis. Membrane proteins or purified rat $G\alpha_{i2}$ protein standard were separated on SDS polyacrylamide gels containing 12% (w/v) acrylamide. Proteins were transferred onto Trans-Blot nitrocellulose membranes (Bio-Rad, Hercules, CA) or onto Immobilon P PVDF membranes (Millipore) and reacted with the M1 anti-FLAG, the anti-$G\alpha_{i1/2}$ or the anti-$G\alpha_o$ antibody (1:1000 each). Protein bands were visualized by enhanced chemoluminescence (Pierce Chemical, Rockford, IL) using goat antimouse IgG (Sigma) or donkey antirabbit IgG (GE Healthcare, Little Chalfont, Buckinghamshire, UK), both coupled to peroxidase. The expression level of proteins was roughly estimated by using appropriate dilutions of reference membranes expressing defined levels of β_2AR or β_2AR-$G\alpha_{i2}$ proteins. β_2AR and β_2AR-$G\alpha_{i2}$ expression levels were determined by radioligand binding with [^{3}H]dihydroalprenolol. Immunoblots were scanned with a GS-710 calibrated imaging densitometer (Bio-Rad). The intensity of the bands was analyzed with the Quantity One 4.0.3 software (Bio-Rad).

Miscellaneous. Protein concentrations were determined with the Bio-Rad DC protein assay kit. Saturation and competition experiments were analyzed by nonlinear regres-

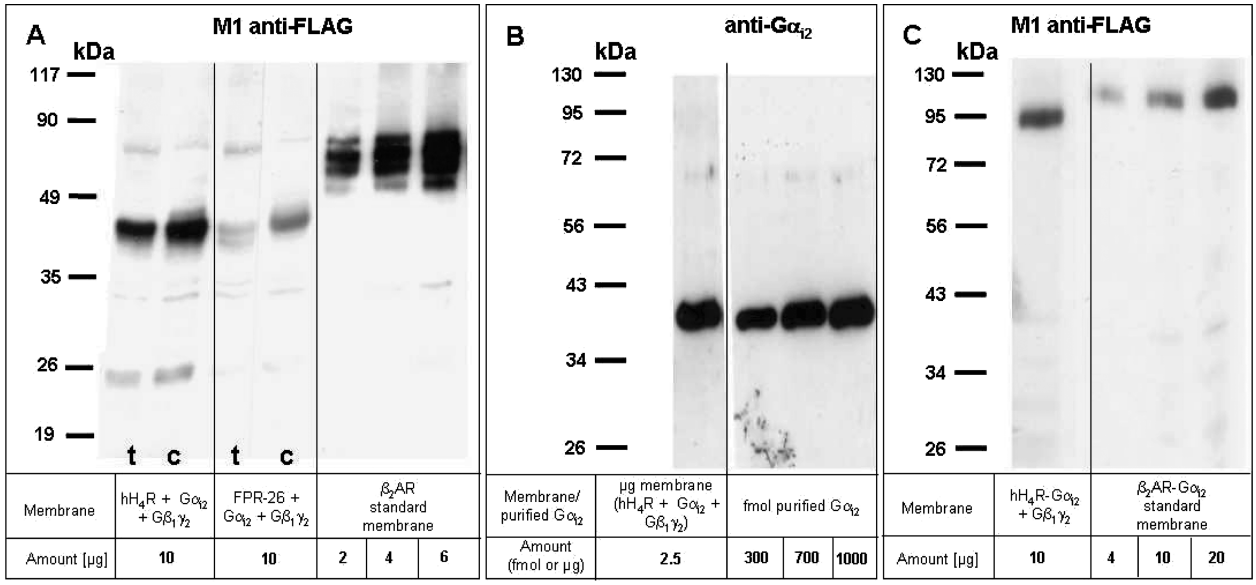

FIGURE 1: Immunoblot analysis of FLAG-hH$_4$R, FLAG-hH$_4$R-Gα_{i2}, and Gα_{i2} expression in Sf9 cell membranes. The amounts of protein loaded onto each lane are given below the membranes. (A) Detection of the hH$_4$R (c, control conditions; t, tunicamycin-treated cell culture) and of the FPR-26 (c, control conditions; t, tunicamycin-treated cell culture) with the M1 monoclonal antibody (anti-FLAG Ig). Three dilutions of a reference membrane, expressing 7.5 pmol/mg FLAG-β_2AR and stained with the M1 antibody, were used for a rough estimation of hH$_4$R expression level (right part of panel A). (B) Detection of the Gα_{i2} protein with the anti-Gα_{i2} antibody and determination of the Gα_{i2} expression level using purified Gα_{i2} protein as a reference. (C) Estimation of the FLAG-hH$_4$R-Gα_{i2} fusion protein expression level with the M1 monoclonal antibody (anti-FLAG Ig) and with a standard membrane expressing 3.5 pmol/mg FLAG-β_2AR-Gα_{i2}. The numbers on the left of each panel indicate the molecular masses of the detected proteins in kDa. All immunoblots were performed as described under Experimental Procedures.

sion with the Prism 4.02 software (GraphPad, San Diego). All values are given as means ± SD. If not stated differently, significance was always calculated using the unpaired two-tailed *t* test and a confidence interval of 95%.

RESULTS

Immunoblotting. We reconstituted the N-terminally FLAG-tagged and C-terminally His$_6$-tagged wild-type hH$_4$R with Gα_{i2} and G$\beta_1\gamma_2$ in Sf9 insect cells. The C-terminus was His$_6$-labeled to protect the receptor against proteolysis and to allow later purification. We also prepared a FLAG-tagged hH$_4$R-Gα_{i2} fusion protein with His$_6$ as a linker in order to enhance G-protein coupling of the receptor and to obtain a defined 1:1 stoichiometry (*31*). The fusion protein was coexpressed with G$\beta_1\gamma_2$.

Expression of hH$_4$R and hH$_4$R-Gα_{i2} was investigated by immunoblotting with the M1 anti-FLAG antibody. The Gα_{i2} protein was detected with a G$\alpha_{i1/2}$-specific antibody. The nonfused hH$_4$R migrated as two bands. A relatively weak band is located at ~46 kDa at the upper border of a very intense hH$_4$R signal at ~43 kDa (Figure 1A, lane 2). The bands in the 30−35 and 26 kDa regions could represent atypically migrating H$_4$R species. A similar pattern of low-molecular species was previously observed for the guinea pig H$_1$ receptor (*32*). The 43 and 46 kDa bands most likely represent different glycosylation states. Glycosylation of the hH$_4$R was previously reported in the literature (*33*).

To investigate hH$_4$R glycosylation in more detail, Sf9 cells expressing hH$_4$R, Gα_{i2}, and G$\beta_1\gamma_2$ were cultured in the presence of tunicamycin, which inhibits protein glycosylation (*28*). The efficiency of the tunicamycin treatment was proven in control experiments performed under the same conditions with membranes expressing FPR-26 (Figure 1A, lanes 3 and 4) or β_2AR (data not shown). Similarly to previously reported results (*28*), the molecular mass of FPR-26 was considerably reduced upon tunicamycin treatment (Figure 1A: lane 3, tunicamycin-treated; lane 4, untreated control). A strong tunicamycin effect was also observed at β_2AR (data not shown).

The weak 46 kDa signal of the hH$_4$R disappeared in the tunicamycin-treated membranes (Figure 1A, lane 1), indicating that it represents a glycosylated hH$_4$R species. A comparably small difference of 2−4 kDa between glycosylated and nonglycosylated hH$_4$R species was previously reported in the literature (*33*). However, in contrast to our results, the intensity of the band of the glycosylated hH$_4$R was markedly higher compared to the nonglycosylated species. This may reflect cell-type specific differences in protein glycosylation, since the experiments in (*33*) were performed with HEK-293 cells instead of Sf9 insect cells.

The expression level of the nonfused hH$_4$R was roughly estimated by comparison with a dilution series of a FLAG-β_2AR (Figure 1A, lanes 5−7) reference membrane. To ensure a comparable blotting efficiency, the reference protein should have a molecular mass comparable to the quantified protein. Therefore, a FLAG-β_2AR-Gα_{i2} membrane was used for the quantitation of the hH$_4$R-Gα_{i2} fusion protein (Figure 1C). The B_{max} values of the reference membranes (7.5 pmol/mg for FLAG-β_2AR and 3.5 pmol/mg for FLAG-β_2AR-Gα_{i2}) were determined by saturation binding with 10 nM of the β_2AR antagonist [^{3}H]dihydroalprenolol ([^{3}H]DHA).

Since all proteins with accessible epitopes are stained by the antibody independently of their folding state, this method also detects nonfunctional receptor protein. The percentage of misfolded receptor protein depends on receptor type. Therefore, the FLAG-β_2AR and FLAG-β_2AR-Gα_{i2} standard membranes should be used with caution to quantify hH$_4$R

Table 1: Comparison of the Pharmacological Properties of the Glycosylated and Tunicamycin (=Tuna)-Treated hH_4R Coexpressed with $G\alpha_{i2}$ and $G\beta_1\gamma_2$, of the hH_4R Expressed in the Absence of Mammalian G Proteins and of the hH_4R-$G\alpha_{i2}$ Fusion Protein Coexpressed with $G\beta_1\gamma_2$[a]

	$hH_4R + G\alpha_{i2} + G\beta_1\gamma_2$	$hH_4R + G\alpha_{i2} + G\beta_1\gamma_2$ + Tuna	hH_4R	hH_4R-$G\alpha_{i2} + G\beta_1\gamma_2$
		Immunoblot		
apparent B_{max} (pmol/mg)	2.7 ± 0.4	2.9 ± 1.5	1.5 ± 0.2	6.1 ± 2.5
		[^{3}H]HA Binding		
no GTPγS (control)				
K_D (nM)	9.7 ± 1.7	9.0 ± 4.8	11.7 ± 2.5	13.6 ± 4.9
B_{max} (pmol/mg)	1.6 ± 0.3	0.3 ± 0.1	2.3 ± 0.2	5.2 ± 1.5
+ 10 μM GTPγS				
K_D (nM)	10.8 ± 5.4	8.9 ± 0.5	13.9 ± 3.8	14.8 ± 2.0
B_{max} (pmol/mg)	1.5 ± 0.5	0.4 ± 0.1	2.9 ± 0.1	5.3 ± 0.1
		[^{35}S]GTPγS Binding		
agonist-stimulated				
K_D (nM)	3.4 ± 1.3	9.6 ± 5.1	n.a.[b]	0.9 ± 0.2
B_{max} (pmol/mg)	2.7 ± 1.0	0.9 ± 0.8	n.a.	1.6 ± 0.3
inverse agonist-inhibited				
K_D (nM)	10.0 ± 4.0	7.2 ± 2.5	n.a.	3.6 ± 0.7
B_{max} (pmol/mg)	5.3 ± 2.1	0.7 ± 0.3	n.a.	4.5 ± 1.3
ΔB_{max} (pmol/mg)	7.9 ± 3.0	1.6 ± 0.9	n.a.	6.0 ± 1.4
coupling factor	4.9 ± 2.7	4.9 ± 4.4	n.a.	1.2 ± 0.6
		GTPase Assay		
agonist-stimulated				
K_m (nM)	357 ± 71	517 ± 182	n.a.	196 ± 23
V_{max} (pmol·(min·mg)$^{-1}$)	4.9 ± 1.0	0.9 ± 0.5	n.a.	1.7 ± 0.1
inverse agonist-inhibited				
K_m (nM)	324 ± 132	356 ± 26	n.a.	274 ± 76
V_{max} (pmol·(min·mg)$^{-1}$)	2.9 ± 0.2	0.5 ± 0.3	n.a.	2.3 ± 0.3
ΔV_{max} (pmol·(min·mg)$^{-1}$)	7.7 ± 0.8	1.4 ± 0.8	n.a.	3.9 ± 0.4
turnover number (min^{-1})	4.4 ± 1.3	4.3 ± 3.7	n.a.	0.9 ± 0.1

[a] All constructs were investigated in immunoblots, [^{3}H]HA binding, [^{35}S]GTPγS binding and steady-state GTPase assay. Data shown are means ± SD of 2−12 independent experiments performed with 1−4 different membrane batches in duplicates or triplicates. [b] n.a., not applicable.

or hH_4R-Ga_{i2}. In the following, the hH_4R B_{max} values from immunoblots are called "apparent" B_{max} values, indicating that this is no exact quantification, but rather an expression level comparable to that of a FLAG-tagged β_{2A}R membrane stained with the same antibody. In Table 1, the apparent B_{max} values from the immunoblots are compared with the corresponding data from [^{3}H]HA binding and [^{35}S]GTPγS saturation binding assays. Apparent B_{max} values from immunoblots are useful to compare different hH_4R-expressing membrane batches. For example, the apparent B_{max} value of the hH_4R calculated from the immunoblot in Figure 1A was ~2 pmol/mg and markedly lower than the corresponding value for hH_4R-$G\alpha_{i2}$ (~7 pmol/mg, Figure 1C). In all studied membrane preparations, the apparent B_{max} of hH_4R was lower compared to hH_4R-$G\alpha_{i2}$. The $G\alpha_{i2}$ subunit fused to the hH_4R may have a chaperone-like function or a stabilizing effect on the receptor protein, increasing the number of properly folded receptors that are inserted in the cell membrane.

For quantitation of $G\alpha_{i2}$ in the membranes, we used purified rat $G\alpha_{i2}$ protein as a reference (Figure 1B). In the case of the immunoblot in Figure 1, we estimated an expression level of ~2 pmol/mg for the nonfused hH_4R (Figure 1A) and 330 pmol/mg for the $G\alpha_{i2}$ subunit (Figure 1B). This is a more than 100-fold excess of G-protein compared to the hH_4R expression level and ensures that the signal transduction of the hH_4R is not compromised by limited availability of G-proteins.

Characterization of the hH4R by Radioligand Binding. The hH_4R (coexpressed with $G\alpha_{i2}$ and $G\beta_1\gamma_2$) had an affinity of 9.7 ± 1.7 nM for [^{3}H]HA in saturation binding experiments. This fits to the range of 5−20 nM reported in the literature (*3*−*5*, *7*). The [^{3}H]HA binding affinity of hH_4R-$G\alpha_{i2}$ (coexpressed with $G\beta_1\gamma_2$) did not differ significantly (Table 1). Interestingly, the K_d value of [^{3}H]HA at the tunicamycin-treated hH_4R (coexpressed with $G\alpha_{i2}$ and $G\beta_1\gamma_2$) was also not significantly altered (Table 1). Thus, receptor glycosylation is of minor importance for the conformation of the hH_4R [^{3}H]HA binding site.

The B_{max} values of membranes expressing only the hH_4R, the hH_4R-$G\alpha_{i2}$ fusion protein in combination with $G\beta_1\gamma_2$, or the hH_4R (glycosylated and deglyosylated) with $G\alpha_{i2}$ and $G\beta_1\gamma_2$ were determined by [^{3}H]HA binding. We recorded complete saturation curves from 1.6 to 100 nM [^{3}H]HA or performed single-point determinations with 100 nM [^{3}H]HA. The [^{3}H]HA binding B_{max} value of the tunicamycin-treated hH_4R was about 75% lower than the B_{max} value obtained from nontreated control membranes (Table 1). This suggests that hH_4R receptor glycosylation is essential for the expression of intact receptors at the cell surface, similar to what was described earlier for FPR-26 (*28*).

Interestingly, for tunicamycin-treated membranes the apparent B_{max} value from immunoblots was ~10-fold higher than the corresponding value from [^{3}H]HA binding. This indicates that the majority of the nonglycosylated hH_4R receptors is misfolded, being recognized by the M1 antibody but not by [^{3}H]HA. In all other membranes (glycosylated hH_4R and hH_4R-$G\alpha_{i2}$ fusion protein), the B_{max} values from radioligand binding and immunoblot were comparable (Table 1).

Radioligand binding experiments were also performed in the presence of 10 μM GTPγS. GTPγS binds to the activated $G\alpha$ subunit instead of GTP but cannot be hydrolyzed (*34*). In general, this causes uncoupling of the receptor from the G-protein, leading to a reduction of the number of high-affinity binding sites (*35*).

Surprisingly, as shown by Figure 2B,C and Table 1, neither the B_{max} nor the K_d value of [^{3}H]HA were altered by GTPγS

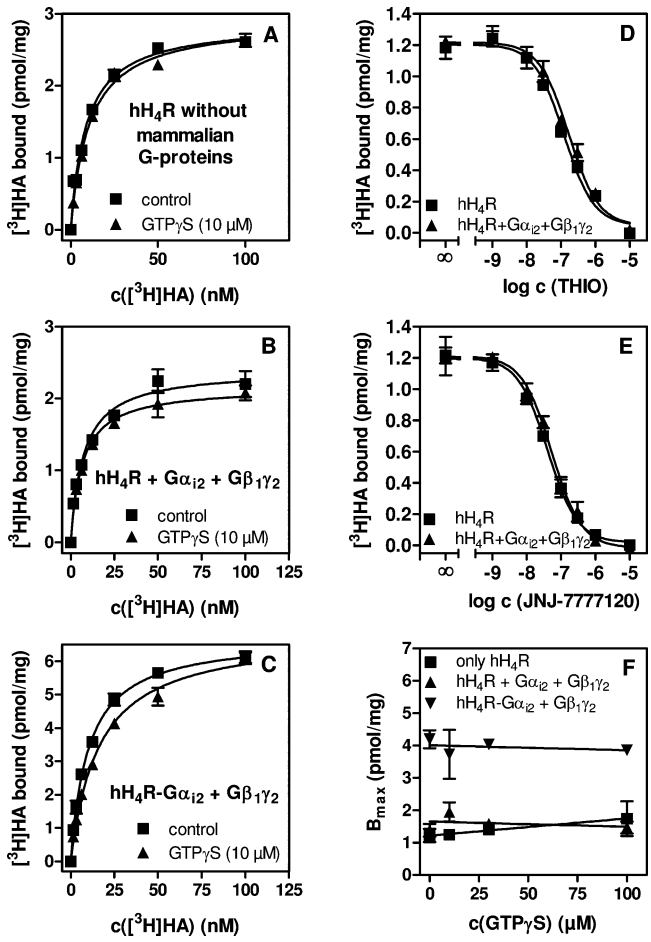

FIGURE 2: [^{3}H]HA radioligand binding assays. (A)−(C) [^{3}H]HA saturation binding curves under control conditions (■) and in the presence of 10 μM GTPγS (▲) at the hH$_4$R in the absence of mammalian G-proteins (A), at the hH$_4$R coexpressed with Gα_{i2} and G$\beta_1\gamma_2$ (B), and at the hH$_4$R-Gα_{i2} fusion protein coexpressed with G$\beta_1\gamma_2$ (C). (D) Displacement curve with the hH$_4$R inverse agonist THIO in the presence of 10 nM [^{3}H]HA, determined with membranes expressing only the hH$_4$R (■) and coexpressing the hH$_4$R with Gα_{i2}G$\beta_1\gamma_2$ (▲). (E) Displacement curve with the hH$_4$R antagonist JNJ-7777120 in the presence of 10 nM [^{3}H]HA, determined with membranes expressing only the hH$_4$R (■) and coexpressing the hH$_4$R with Gα_{i2}G$\beta_1\gamma_2$ (▲). (F) Influence of increasing GTPγS concentrations on the B_{max} value (specific binding of 100 nM [^{3}H]HA) of membranes expressing only the hH$_4$R (■), coexpressing the hH$_4$R with Gα_{i2} and G$\beta_1\gamma_2$ (▲), or coexpressing the hH$_4$R-Gα_{i2} fusion protein with G$\beta_1\gamma_2$ (▼). All data shown are means ± SD of one representative experiment with 2−3 replicates, as described under Experimental Procedures. Similar data were obtained from 2−3 experiments with 2−3 replicates.

in membranes expressing nonfused hH$_4$R (+Gα_{i2} + G$\beta_1\gamma_2$) and hH$_4$R-Gα_{i2} (+G$\beta_1\gamma_2$). Also the tunicamycin-treated hH$_4$R was insensitive to GTPγS (Table 1). In order to exclude the possibility that the observed GTPγS resistance was due to filter binding effects, we performed competition binding assays with the antagonist JNJ-7777120 and the inverse agonist THIO. Specifically bound [^{3}H]HA was readily displaced, resulting in a K_i value of 106 ± 21 nM for THIO (Figure 2D) and 32 ± 7 nM for JNJ-7777120 (Figure 2E). These affinities agree well with literature data (*10*) and show the specificity of the observed binding. Moreover, no displaceable [^{3}H]HA binding was observed in membranes expressing only Gα_{i2} and G$\beta_1\gamma_2$ (data not shown).

We also investigated membranes expressing only hH$_4$R in the absence of any coexpressed mammalian G-protein (Figure 2A). Surprisingly, the K_d value of [^{3}H]HA did not differ significantly from the K_d value determined with membranes expressing hH$_4$R in the presence of Gα_{i2} and G$\beta_1\gamma_2$ (Table 1). The K_i values of JNJ-7777120 and THIO were also not altered in the absence of G-proteins (Figure 2D,E). GTPγS (10 μM) did not change the B_{max} value and the binding affinity of [^{3}H]HA in this system (Figure 2A and Table 1). It is very unusual to observe high-affinity agonist-binding and even more unusual to observe GTPγS-resistant high-affinity agonist binding at a GPCR expressed in Sf9 cells without coexpressed mammalian G-proteins (*36*).

GTPγS Saturation Binding. We performed [^{35}S]GTPγS saturation binding experiments with GTPγS concentrations from 0.1−25 nM in membranes expressing only the hH$_4$R (Table 1, Figure 3A), coexpressing the hH$_4$R with Gα_{i2} and G$\beta_1\gamma_2$ (Table 1, Figure 3C), or the hH$_4$R-Gα_{i2} fusion protein with G$\beta_1\gamma_2$ (Table 1, Figure 3E). Moreover, [^{35}S]GTPγS saturation binding was investigated with membranes coexpressing the tunicamycin-treated hH$_4$R with Gα_{i2} and G$\beta_1\gamma_2$ (Table 1). Membranes were incubated for 240 min in the presence of HA (10 μM) or THIO (10 μM) or under control conditions (H$_2$O). In Figure 3A,C,E, the control curve was subtracted from the GTPγS binding curves determined in the presence of HA and THIO. This enables the calculation of GTPγS binding affinity to Gα_{i2}, regulated by the agonist-stimulated or the constitutively active receptor.

When the nonfused hH$_4$R (coexpressed with Gα_{i2} and G$\beta_1\gamma_2$, Figure 3C and Table 1) was stimulated with the agonist HA, we found an apparent K_d value of 3.4 ± 1.3 nM for GTPγS at the Gα_{i2} protein. Uncoupling of hH$_4$R from the G-protein by the inverse agonist THIO significantly ($p < 0.01$) increased the apparent GTPγS K_d value by about 3-fold (Table 1). The apparent GTPγS K_d value at Gα_{i2} coupling to the hH$_4$R in tunicamycin-treated membranes was significantly increased ($p < 0.01$) under agonist-stimulated conditions, compared to the K_d value in the presence of glycosylated hH$_4$R. This indicates that, despite marked constitutive activity and the presence of the agonist HA, the tunicamycin-treated hH$_4$R is less effective at activating the Gα_{i2} subunit. In the presence of THIO, the apparent GTPγS K_d value at Gα_{i2} did not differ significantly between the membranes expressing glycosylated and tunicamycin-treated hH$_4$R. In the hH$_4$R-Gα_{i2} fusion protein (coexpressed with G$\beta_1\gamma_2$), the K_d value of GTPγS was significantly decreased compared to the coexpression system ($p < 0.01$) in the presence of both HA and THIO (Figure 3E, Table 1). This reflects a more efficient hH$_4$R/Gα_{i2} interaction in the hH$_4$R-Gα_{i2} fusion protein compared to the coexpression system. No significant GTPγS binding was determined when hH$_4$R was expressed without mammalian G-proteins (Figure 3A). This confirms that the signal in the presence of Gα_{i2} and G$\beta_1\gamma_2$ is due to an efficient interaction of hH$_4$R with the mammalian G-proteins.

As described previously (*28, 37*), GTPγS binding assays also provide information on the number of Gα subunits activated by the agonist-stimulated receptor (Table 1) and the constitutively active receptor (Table 1, inverse agonist-inhibited). The sum of both B_{max} values is the number of Gα subunits totally regulated by the receptor (Table 1,

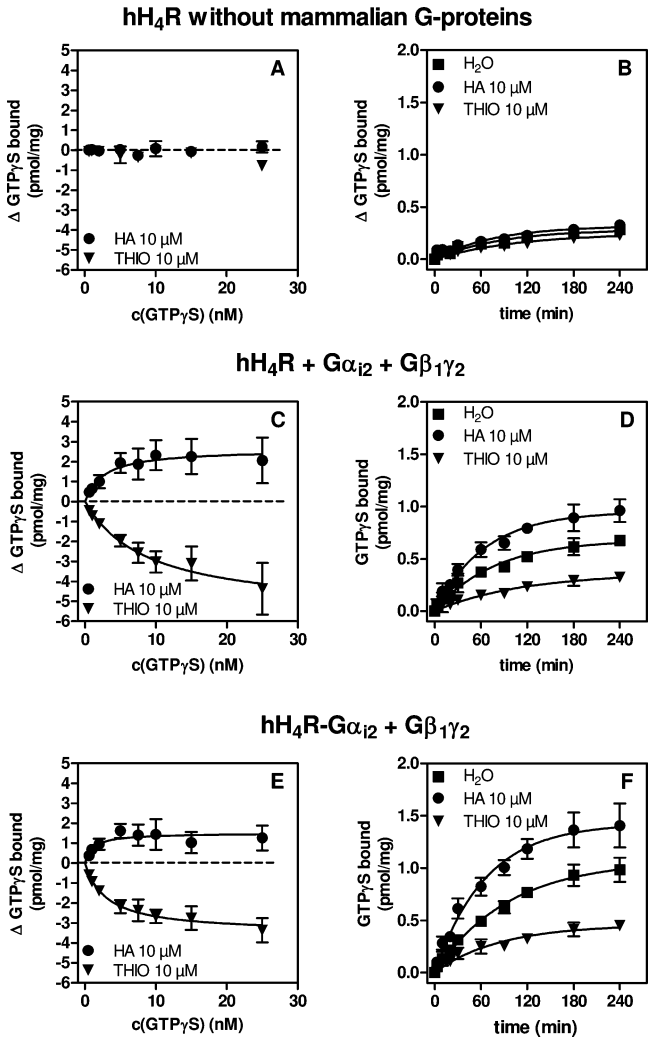

FIGURE 3: [^{35}S]GTPγS binding assays. [^{35}S]GTPγS saturation binding and time course experiments with Sf9 cell membranes expressing the hH_4R without mammalian G-proteins (A, B), coexpressing the hH_4R with $G\alpha_{i2}$ and $G\beta_1\gamma_2$ (C, D), or coexpressing the hH_4R-$G\alpha_{i2}$ fusion protein with $G\beta_1\gamma_2$ (E, F). For each membrane, the saturation binding experiments are shown on the left (A, C, E) and the time course experiments are shown on the right (B, D, F). All reaction mixtures contained 1 μM GDP. Determination of constitutive activity (■) and HA-stimulated (●) and THIO-inhibited (▼) [^{35}S]GTPγS binding. HA and THIO were used in a concentration of 10 μM each. For the saturation binding experiments (A, C, E), the samples were incubated for 240 min at 25 °C. The GTPγS bound under control conditions was subtracted from the GTPγS bound in the presence of HA or THIO, in order to obtain the HA-induced G-protein activation, and the spontaneous G-protein activation blocked by THIO. All data shown (except for (A), one representative experiment in duplicates) are means ± SD of 2−6 experiments in duplicates. All experiments were performed as described under Experimental Procedures.

ΔB_{max}). Dividing the total number of activated $G\alpha_{i2}$ proteins by the B_{max} value from [^{3}H]HA binding results in the coupling factor (Table 1) and reveals catalytic signaling of the hH_4R in the coexpression system with $G\alpha_{i2}$ and $G\beta_1\gamma_2$. One hH_4R receptor activates ∼4−5 $G\alpha_{i2}$ proteins. Tunicamycin-treatment did not change the coupling factor of the hH_4R, suggesting that glycosylation does not influence the colocalization of hH_4R with G proteins in Sf9 cell membranes. The coupling factor of hH_4R-$G\alpha_{i2}$ was ∼1 (Table 1), indicating that the hH_4R only activates the fused $G\alpha_{i2}$ protein, but no insect cell G-proteins. This is in agreement with the data obtained for other GPCR-Gα fusion proteins in our laboratory (*31, 38*).

About 70% of the totally ligand-regulated $G\alpha_{i2}$ proteins are constitutively activated by the agonist-free receptor in both coexpression and the fusion protein system. Interestingly, this constitutive activity is higher than in the GTPase assay (40−55%, Figure 7). At first glance, this seems to be contradictory, but these discrepancies may be explained by the structural differences between GTP and GTPγS (small γ-phosphate oxygen versus bulky γ-phosphate sulfur), resulting in different binding modes to G-proteins. In fact, a previous study from our laboratory already demonstrated striking differences in the interaction of G_s-protein mutants with xanthosine 5′-triphosphate and xanthosine 5′-[γ-thio]triphosphate (*39*).

In contrast to previously reported results for the FPR-26 (*28*), the tunicamycin-treated hH_4R still shows considerable constitutive activity in GTPγS saturation binding (∼40%), which is reduced compared to the control membrane (∼70%). This difference indicates that the constitutive activities of the hH_4R and FPR-26 are caused by different conformational changes in receptor structure. This is also corroborated by the differing behavior of hH_4R and FPR in the presence of GTPγS and NaCl (*21*).

GTPγS Binding Kinetics. We determined the binding kinetics of [^{35}S]GTPγS (0.4 nM) to $G\alpha_{i2}$ in coexpression membranes (hH_4R + $G\alpha_{i2}$ + $G\beta_1\gamma_2$), in fusion protein membranes (hH_4R-$G\alpha_{i2}$ + $G\beta_1\gamma_2$), and in background membranes (only hH_4R). All experiments were performed under control conditions (H_2O) and in the presence of HA (10 μM) or THIO (10 μM). The signal in the background membranes expressing hH_4R without mammalian G-proteins was very low (Figure 3B), indicating that there is no relevant GTPγS binding to insect cell G-proteins. In contrast, in coexpression membranes (hH_4R + $G\alpha_{i2}$ + $G\beta_1\gamma_2$) a clear signal was detected (Figure 3D), showing an efficient hH_4R/$G\alpha_{i2}$ interaction. However, the $G\alpha_{i2}$ subunit was activated very slowly (Figure 3D). The time until 50% of the maximum effect was approached ($t_{1/2}$) was 53 ± 8 min under control conditions, 45 ± 7 min in the presence of HA, and 85 ± 33 min in the presence of THIO. The $G\alpha_{i2}$ protein in the hH_4R-$G\alpha_{i2}$ fusion protein showed very similar GTPγS binding kinetics with $t_{1/2}$ values of 67 ± 17, 46 ± 9, and 64 ± 25 min for control conditions, HA (10 μM), and THIO (10 μM), respectively (Figure 3F).

The GTPγS binding kinetics revealed very high constitutive activity of the H_4R. The relative signals of HA and THIO were about + 50% and −50%, respectively, with no difference between the coexpression system and the hH_4R-$G\alpha_{i2}$ fusion protein. Despite the slow binding kinetics of GTPγS, the relative signals of HA and THIO remained constant after 90 min.

In reporter gene assays, THIO inhibited the spontaneous hH_4R activity in hH_4R-transfected SK-N-MC cells to the same extent as treatment with pertussis toxin and was referred to as full-inverse agonist with an efficacy of −1.00 (*10*). However, it is very difficult if not impossible to ADP-ribosylate all G_i-proteins by pertussis toxin in intact cells (*40*). Therefore, we prepared a membrane coexpressing the hH_4R with $G\alpha_{i2}$ and $G\beta_1\gamma_2$ and an hH_4R-free background membrane, expressing only $G\alpha_{i2}$ and $G\beta_1\gamma_2$. We performed GTPγS binding assays in the presence of THIO and under

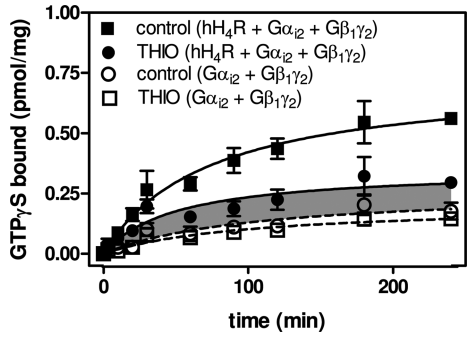

FIGURE 4: Determination of the absolute effect of THIO in GTPγS binding kinetics. The THIO effect was determined using membranes coexpressing the hH_4R with $G\alpha_{i2}$ and $G\beta_1\gamma_2$ (●) and with membranes expressing only $G\alpha_{i2}$ and $G\beta_1\gamma_2$ (□). The control curve was determined with membranes expressing the hH_4R, $G\alpha_{i2}$, and $G\beta_1\gamma_2$ (■) and expressing only $G\alpha_{i2}$ and $G\beta_1\gamma_2$ (○). The gray area shows the GTPγS binding that was not inhibited by THIO. All data shown are means ± SD from two experiments in triplicates, performed with a membrane pair from the same membrane preparation. All experiments were performed as described under Experimental Procedures.

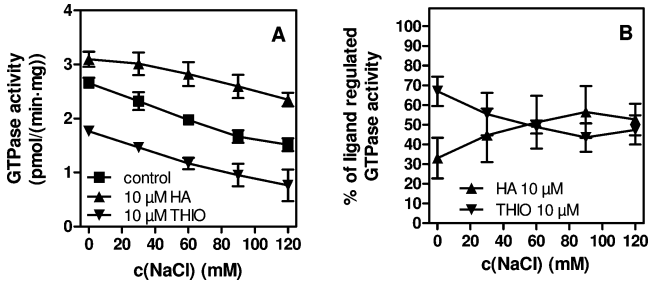

FIGURE 5: Effect of NaCl on hH_4R-induced GTPase activity. Effects of NaCl on steady-state GTPase activity were studied under control conditions (■), with HA-stimulation (▲), and with THIO-inhibition (▼) in Sf9 cell membranes expressing the hH_4R with $G\alpha_{i2}$ and $G\beta_1\gamma_2$. HA and THIO were used at a concentration of 10 μM each. The GTPase assay was performed as described under Experimental Procedures. (A) Absolute GTPase activities. (B) Percentage of HA and THIO effects, related to total ligand-regulated GTPase activity. Data shown are means ± SD of three experiments performed in triplicates (one membrane). Resistance of the R state to 100 mM of Na^+ was confirmed with other membranes from four independent preparations.

control conditions. Despite the presence of 100 mM of NaCl, which additionally reduces the constitutive activity, THIO was not able to reduce GTPγS binding in the coexpression membrane (hH_4R + G-proteins) to the same extent as in the background membrane (Figure 4). This indicates that THIO is only a partial inverse agonist at the hH_4R.

Influence of NaCl on Constitutive hH4R Activity in Steady-State GTPase Assays. The hH_4R is constitutively active and THIO acts as an inverse agonist (*4, 5, 10*). Na^+ stabilizes the inactive R state of many GPCRs and reduces the basal activity. This was described, e.g.,for the FPR-26 and the α_2-adrenergic receptor (*41, 42*). We investigated the effect of NaCl on the constitutive activity of the hH_4R coexpressed with $G\alpha_{i2}$ and $G\beta_1\gamma_2$ in steady-state GTPase assays. For each NaCl concentration the constitutive activity, the effects of HA (10 μM) and of THIO (10 μM) were determined.

As shown in Figure 5A, in the absence of NaCl, the hH_4R showed a pronounced constitutive activity with a relative stimulatory HA signal of only 17%. The inverse agonist THIO reduced the constitutive activity by 34%. Surprisingly,

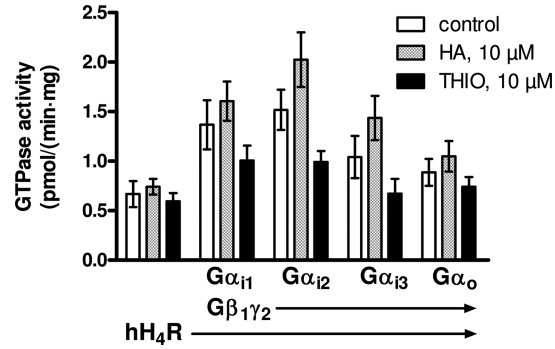

FIGURE 6: Coupling efficiency of the hH_4R to G-protein subtypes of the $G\alpha_{i/o}$ class. The hH_4R was coexpressed with $G\beta_1\gamma_2$ and various G-protein subunits of the $G\alpha_{i/o}$ class ($G\alpha_{i1}$, $G\alpha_{i2}$, $G\alpha_{i3}$, and $G\alpha_o$). As a control, the hH_4R was expressed in the absence of mammalian G-proteins. G-protein coupling efficiency was determined by steady-state GTPase assay. Every group of three bars in the diagram represents the results for one specific membrane under control conditions (bar 1), in the presence of agonist (HA, 10 μM, bar 2), and in the presence of inverse agonist (THIO, 10 μM, bar 3). The proteins expressed in the different membranes are shown below the diagram. The data represent means ± SD of two independent assays (one membrane batch, 3−4 replicates).

increasing concentrations of NaCl had only a minor effect on the inverse-agonistic activity of THIO (Figure 5B). As shown in Figure 5B, the relative effect of HA was increased in the presence of NaCl. Therefore, we added 100 mM NaCl to all functional assays (steady-state GTPase and GTPγS binding) to obtain a higher signal-to-background ratio for agonist-induced signals. Since the inverse agonistic effect of THIO was retained under these conditions, this system is suited for both the pharmacological characterization of agonists and inverse agonists.

Analysis of hH4R G-Protein Coupling Selectivity. Based on the relatively small agonist-induced stimulation of GTP hydrolysis compared to other $G\alpha_i$-coupled receptors, such as FPR-26 (*21*) or CXCR4 (*43*), the question arose whether $G\alpha_{i2}$ is the optimal G-protein for the hH_4R, and whether the receptor may couple more effectively to other Gα subtypes. Therefore, we coexpressed hH_4R with $G\alpha_{i1}$, $G\alpha_{i2}$, $G\alpha_{i3}$, and $G\alpha_o$ in combination with $G\beta_1\gamma_2$. The expression of G-proteins was determined by using an anti-$G\alpha_{i1/2}$ and the anti-$G\alpha_o$ antibody (data not shown). To assess the background signal, the hH_4R was also expressed without mammalian G proteins. We determined the constitutive activity and the effects of HA (10 μM) or THIO (10 μM) in the steady-state GTPase assay.

The results are shown for a batch of membranes prepared on the same day under the same conditions (Figure 6). Statistical significance of differences in steady-state GTPase activity was calculated with one-way ANOVA followed by Dunnet's multiple comparison test. Under all conditions (control, HA, or THIO), steady-state GTPase activity was significantly increased ($p < 0.01$) in the presence of $G\alpha_{i2}$, compared to the control membrane (only hH_4R), or to the membranes expressing $G\alpha_{i3}$ or $G\alpha_o$. Compared to $G\alpha_{i1}$, the steady-state GTPase activity of hH_4R-stimulated $G\alpha_{i2}$ was only significantly higher ($p < 0.01$) when the receptor was stimulated with HA. $G\alpha_o$ was hardly stimulated by hH_4R, and the observed signals were only significantly increased compared to the control membrane (only hH_4R) in the presence of HA. Taken together, our results show a preference of the hH_4R for $G\alpha_{i2}$, immediately followed by $G\alpha_{i1}$.

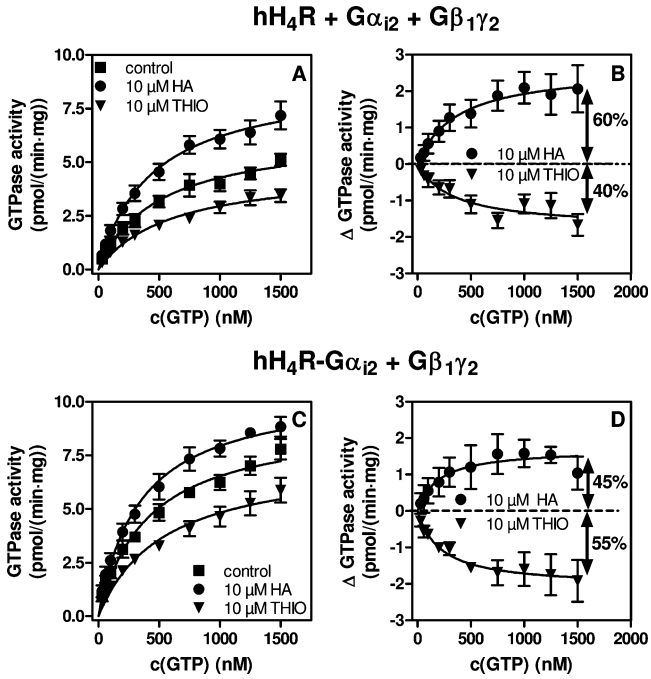

FIGURE 7: hH_4R-mediated modulation of $G\alpha_{i2}$ GTPase enzyme kinetics. The K_m value of the $G\alpha_{i2}$ GTPase activity was determined by steady-state GTPase assay in Sf9 cell membranes coexpressing the hH_4R with $G\alpha_{i2}$ and $G\beta_1\gamma_2$ or coexpressing the hH_4R-$G\alpha_{i2}$ fusion protein with $G\beta_1\gamma_2$. The diagrams show the constitutive activity (■) as well as the effect of HA (●) and THIO (▼). HA and THIO were used in a concentration of 10 μM each. (A, B) GTPase activity in dependency on the GTP concentration, determined with the coexpression system (hH_4R + $G\alpha_{i2}$ + $G\beta_1\gamma_2$) without (A) and with (B) baseline subtraction. (C, D) Plots of steady-state GTPase activity in dependency on the GTP concentration, determined with the fusion protein system (hH_4R-$G\alpha_{i2}$ + $G\beta_1\gamma_2$) without (C) and with (D) baseline subtraction. All data shown are means ± SD of four experiments performed in triplicates with two different membranes. All experiments were performed as described under Experimental Procedures.

GTPase Kinetics. The affinity of $G\alpha_{i2}$ for GTP was investigated by determination of steady-state GTPase activity in the presence of increasing GTP concentrations (Figure 7). All experiments were performed under control conditions and in the presence of HA (10 μM) or THIO (10 μM). Comparison of panels A (hH_4R + $G\alpha_{i2}$ + $G\beta_1\gamma_2$) and C (hH_4R-$G\alpha_{i2}$ + $G\beta_1\gamma_2$) of Figure 7shows that absolute GTPase activitiy is increased in the case of hH_4R-$G\alpha_{i2}$ under all conditions (control, HA, or THIO).

In panels B (hH_4R + $G\alpha_{i2}$ + $G\beta_1\gamma_2$) and D (hH_4R-$G\alpha_{i2}$ + $G\beta_1\gamma_2$) of Figure 7, the control curve was subtracted from the HA and THIO curve. This allows for the determination of the apparent K_m value of GTP at the $G\alpha_{i2}$ subunit stimulated by the agonist-activated (HA) or by the constitutively active receptor (THIO). Neither in the coexpression system nor in the fusion protein system did THIO reduce the K_m value of $G\alpha_{i2}$ for GTP. This indicates that THIO mainly has an effect on the V_{max} of the GTPase reaction.

Compared to the corresponding K_m value from the coexpression system, the apparent K_m value of GTP at hH_4R-$G\alpha_{i2}$ was significantly decreased ($p < 0.01$) in the presence of HA. The K_m value at hH_4R-$G\alpha_{i2}$ in the presence of THIO was slightly but not significantly reduced compared to the coexpression system. This corroborates the results from GTPγS saturation binding, where the affinity of GTPγS was enhanced in the fusion protein system, compared to the coexpression system. In the tunicamycin-treated coexpression membranes (hH_4R + $G\alpha_{i2}$ + $G\beta_1\gamma_2$), the GTP affinities in the presence of HA and THIO did not significantly differ from the corresponding affinities in the untreated membranes. All K_m- and V_{max} values are listed in Table 1.

From Figure 7B,D, the total ligand-regulated GTPase activity as well as the percentage of constitutive activity and HA-induced stimulation was calculated. Although the hH_4R-$G\alpha_{i2}$ expression level was considerably higher than the B_{max} of the nonfused hH_4R (cf. Table 1), the total ligand-regulated GTPase activity in the fusion protein membranes was lower compared to the coexpression system (Table 1). When the total receptor-regulated GTPase activity is divided by the [^{3}H]HA binding B_{max} value, the GTPase-activity, which is regulated by a single receptor molecule (turnover number), can be calculated. We obtained a turnover number of 0.9 min^{-1} for the hH_4R-$G\alpha_{i2}$ fusion protein (+$G\beta_1\gamma_2$) and of 4.4 min^{-1} for the coexpression system (hH_4R + $G\alpha_{i2}$ + $G\beta_1\gamma_2$). The turnover number of tunicamycin-treated coexpression membranes did not significantly differ from the turnover number of solvent-treated control membranes. This confirms the coupling factors determined in GTPγS binding shown in Table 1.

The percentage of constitutive steady-state GTPase activity related to the total receptor-regulated activity is increased from ~40% in the coexpression system to ~55% in the hH_4R-$G\alpha_{i2}$ fusion protein system (Figure 7B,D). In return, the proportion of the signal induced by HA (10 μM) is reduced from 60% (coexpression system) to 45% (fusion protein system). This reflects a more efficient interaction between the hH_4R and $G\alpha_{i2}$ in the fusion protein. The percentage of constitutive steady-state GTPase activity was ~35% in the tunicamycin-treated coexpression membranes (hH_4R + $G\alpha_{i2}$ + $G\beta_1\gamma_2$).

Influence of THIO and HA on Structural Instability of the hH_4R and the hH_4R-$G\alpha_{i2}$ Fusion Protein. As previously reported for the constitutively active mutant of the β_2AR (β_2AR_{CAM}), high constitutive activity may reduce conformational stability of a GPCR (*29*). This effect can be compensated by the addition of receptor ligands to cell cultures expressing the GPCR (*29*). Considering the high constitutive activity of the hH_4R, we investigated whether addition of hH_4R ligands to baculovirus-infected Sf9 cells influences receptor expression levels. Specifically, Sf9 cell cultures were infected with baculoviruses encoding the nonfused hH_4R (+$G\alpha_{i2}$ + $G\beta_1\gamma_2$) and with viruses for the hH_4R-$G\alpha_{i2}$ fusion protein (+$G\beta_1\gamma_2$). Mini-membrane preparations were performed as described in the Experimental Procedures section, and the B_{max} value of [^{3}H]HA binding (100 nM) was determined. When the coexpression system (hH_4R + $G\alpha_{i2}$ + $G\beta_1\gamma_2$) was considered, membranes prepared from cells cultured in the presence of HA (10 μM) or THIO (1 μM) showed significantly higher B_{max} values than control (H_2O) membranes (Table 2). However, in immunoblots with the M1 anti-FLAG antibody no differences in hH_4R protein expression were found (data not shown). This is in agreement with data obtained for β_2AR_{CAM} (*29*) and indicates that the stabilizing effect of hH_4R ligands is mainly due to a conformational stabilization of membrane-integrated receptor but not due to an increased expression of receptor protein. In marked contrast, HA and THIO showed only a

Table 2: Effect of THIO and HA on B_{max} of hH_4R and of hH_4R-$G\alpha_{i2}$ Fusion Protein Expression[a]

proteins	prep no.	B_{max} (control) (pmol/mg)	B_{max}(HA) (pmol/mg)	B_{max}(THIO) (pmol/mg)	% change of B_{max}
hH_4R	1[b]	1.2 ± 0.2	n.d.[c]	2.9 ± 0.2	+142 (THIO)
	2	0.9 ± 0.1	n.d.	1.6 ± 0.1	+78 (THIO)
$G\alpha_{i2}$	3	0.6 ± 0.1	1.0 ± 0.1	n.d.	+67 (HA)
	4	0.6 ± 0.1	1.6 ± 0.1	n.d.	+167 (HA)
$G\beta_1\gamma_2$	5	1.1 ± 0.2	1.5 ± 0.1	1.4 ± 0.1	+36 (HA)
					+27 (THIO)
hH_4R-$G\alpha_{i2}$	1[b]	4.8 ± 0.1	n.d.	5.1 ± 0.2	+6 (THIO)
	2	2.3 ± 0.1	n.d.	2.7 ± 0.1	+17 (THIO)
	3	2.3 ± 0.2	2.2 ± 0.1	n.d.	−4 (HA)
$G\beta_1\gamma_2$	4	2.2 ± 0.1	2.1 ± 0.1	n.d.	−5 (HA)
	5	1.9 ± 0.4	2.5 ± 0.2	2.0 ± 0.1	+32 (HA)
					+5 (THIO)

[a] All data with the same preparation number (prep no.) were obtained using membranes that were all prepared on the same day under the same conditions. Unless indicated otherwise, all B_{max} values were determined with 100 nM [^{3}H]HA. Experiments were performed as described under Experimental Procedures. Data are means ± SD of one assay in triplicate. [b] Complete saturation curve in duplicate (3.13−100 nM). [c] n.d., not determined.

small if any stabilizing effect on B_{max} of [^{3}H]HA binding when the fusion protein system (hH_4R-$G\alpha_{i2}$ + $G\beta_1\gamma_2$) was considered (Table 2). Interestingly, under control conditions, the [^{3}H]HA binding B_{max} of hH_4R-$G\alpha_{i2}$ was always higher compared to the nonfused hH_4R. Unlike the nonfused hH_4R, also an increased apparent B_{max} value was found in immunoblots (Table 1). It is conceivable that the $G\alpha_{i2}$ subunit in the hH_4R-$G\alpha_{i2}$ fusion enhances receptor stability or reduces protein degradation. Another possible explanation is a chaperone-like action of $G\alpha_{i2}$ in the fusion protein, facilitating correct folding of the hH_4R. This leads to an increase in amount of membrane-integrated correctly folded receptor protein. In contrast, hydrophilic ligands like HA and THIO are incapable of crossing the plasma membrane. Thus, when added to the cell culture medium, these ligands can only biochemically stabilize receptor molecules, which are already successfully inserted in the membrane. This could explain why hH_4R ligands do not further increase the expression level of the hH_4R-$G\alpha_{i2}$ fusion protein.

Stabilizing Effect of THIO and HA on the hH4R in 37 °C Stability Assays. Membrane-permeable receptor ligands can bind to receptor proteins in the endoplasmic reticulum and assist protein folding by stabilizing the correct receptor conformation. Thereby, they increase the amount of receptor molecules integrated into the cell membrane. This effect is also called "pharmacological chaperoning" and was, e.g., reported for the vasopressin V2 receptor (*44*). To perform experiments under conditions in which pharmacological chaperoning is not possible any more, we performed stability assays with isolated membranes coexpressing the hH_4R with $G\alpha_{i2}$ and $G\beta_1\gamma_2$. The membranes were incubated at 37 °C under control conditions (H_2O) or in the presence of HA (10 μM) or THIO (10 μM). By immunoblotting of the membranes after the incubation, we ensured that differences in [^{3}H]HA binding B_{max} values between control, HA-treated, and THIO-treated membranes were not caused by a different extent of enzymatic degradation (data not shown).

The B_{max} value of [^{3}H]HA (100 nM) was used as a measure of conformational integrity of the receptor. As shown in Figure 8A, after 120 min of incubation at 37 °C, only 30% of the original [^{3}H]HA B_{max} value was retained, indicating high conformational instability of the hH_4R. HA enhanced the stability, as indicated by the more than 2-fold higher B_{max} value after 120 min (65%, Figure 8A). Surprisingly, THIO reproducibly led to B_{max} values that were 30−40% higher

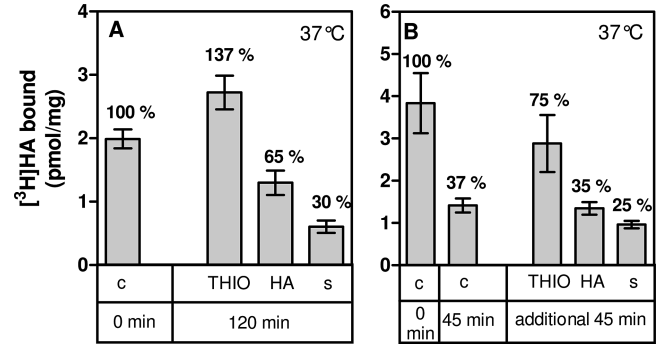

FIGURE 8: Analysis of conformational instability and ligand-mediated stabilization of the hH_4R. (A) Effect of hH_4R ligands on a membrane coexpressing the hH_4R with $G\alpha_{i2}$ and $G\beta_1\gamma_2$. [^{3}H]HA B_{max} values were determined after 120 min of incubation at 37 °C under control conditions (solvent, s) and in the presence of 10 μM of HA or THIO. The numbers above the bars indicate the percentage of intact [^{3}H]HA binding sites compared to the B_{max} of the control sample at the very beginning of the incubation (c, 0 min). The data represent means ± SD from two independent experiments performed in triplicate with two different membranes. (B) Effect of hH_4R ligands on a preincubated membrane coexpressing the hH_4R with $G\alpha_{i2}$ and $G\beta_1\gamma_2$. First, the membrane was incubated without any ligand for 45 min at 37 °C, leading to a reduction of the B_{max} value from 100% (c, 0 min) to 37% (c, 45 min). Thereafter, HA (10 μM), THIO (10 μM), or binding buffer (solvent, s) were added to the membrane and incubation was continued for another 45 min at 37 °C. The numbers above the bars indicate the percentage of intact [^{3}H]HA binding sites compared to the original B_{max} from the very beginning of the incubation (c, 0 min). Data are means ± SD from one representative experiment performed in triplicates.

than the starting value, even after 120 min of incubation at 37 °C. This suggests that THIO may refold a priori-misfolded [^{3}H]HA receptors in the membrane.

To investigate this effect in more detail, membranes coexpressing the hH_4R with $G\alpha_{i2}$ and $G\beta_1\gamma_2$ were first incubated for 45 min at 37 °C, reducing the B_{max} value to 37% of the starting value (Figure 8B). Thereafter, aliquots of this preincubated membrane were incubated for another 45 min at 37 °C in the presence of buffer (solvent control) and of HA (10 μM) or THIO (10 μM). HA stopped the loss of binding sites, and even after the second incubation at 37 °C, there was still 35% of the original B_{max} value retained (Figure 8B). In contrast, in the control sample the B_{max} value was further reduced to 25%, which indicated an ongoing loss of [^{3}H]HA binding sites. Interestingly, THIO really refolded a fraction of the receptor molecules in the second 45 min

Table 3: Potency and Efficacy of Various hH_4R Standard Ligands[a]

	hH_4R in Sf9 cells		literature (*10*)[b]	
	EC_{50} (nM)	efficacy	EC_{50} (nM)	efficacy
HA	13.0 ± 6.3	1.00	20.0	1.0
imetit	6.7 ± 5.2	0.69 ± 0.15	12.6	0.9
immepip	44.4 ± 13.7	0.68 ± 0.15	15.9	0.9
R-α-methylhistamine	277 ± 96	0.92 ± 0.01	631	1.0
5-methylhistamine	32.3 ± 8.1	0.87 ± 0.01	39.8	1.0
iodophenpropit	n.a.[c]	0.00	n.a.	0.0
THIO	95.5 ± 41.9	−1.00[d]	100	−1.0
JNJ-7777120	37.7 ± 8.5	-0.31 ± 0.07	n.a.	0.0

[a] The data were determined in the steady-state GTPase assay using membranes from Sf9 cells co-expressing the hH_4R, $G\alpha_{i2}$ and $G\beta_1\gamma_2$. All experiments were performed as described under Experimental Procedures. The results are compared with data from the literature (*10*). All data are shown as the mean ± SD from 3−5 experiments performed in triplicate (HA, $n = 9$, in triplicate). [b] The pEC_{50}values reported in ref (*10*) were converted to the nonlogarithmic EC_{50} values shown in the table. [c] n.a., not applicable. [d] THIO was used as a reference with an efficacy set to −1. However, it should be noted that THIO acts only as a partial inverse agonist with a "true" efficacy between 0 and −1.

incubation period by increasing the percentage of binding sites from 37% (pre-inactivated membrane) to 75% of the original B_{max} value (Figure 8B). We also recorded the time course of denaturation for the hH_4R and the hH_4R-$G\alpha_{i2}$ fusion protein at 37 °C and obtained a half-life of ∼20 min in both cases (data not shown).

Pharmacological Characterization of the hH_4R Reconstituted in Sf9 Cells. The high constitutive activity of the hH_4R in our expression system enabled us to investigate both agonism and inverse agonism at the hH_4R. To ensure that the hH_4R reconstituted with $G\alpha_{i2}$ and $G\beta_1\gamma_2$ shows full functionality, we determined the potency and efficacy of several standard ligands in the steady-state GTPase assay and compared the results with data from reporter gene assays in the literature (*10*). The EC_{50} and efficacy values and the data from literature are summarized in Table 3.

Overall, there was good agreement in the potencies of agonists (histamine, imetit, immepip, Rα-methylhistamine and 5-methylhistamine) and the inverse agonist THIO between our system and the reporter gene assay (CRE-β-galactosidase) used by Lim et al. (*10*). However, we noticed that the efficacies of imetit, immepip, Rα-methylhistamine and 5-methylhistamine were higher in the gene reporter assay than in the GTPase assay. This difference may reflect the fact that the GTPase assay monitors receptor activation at a much more proximal point than the gene reporter assay, i.e. downstream signal amplification masks subtle differences in ligand efficacy.

Iodophenpropit turned out to be a neutral antagonist in our assay system, which is also consistent with the results from the literature. Interestingly, we found that JNJ7777120, in contrast to the data of Lim et al. (*10*), is not a neutral antagonist but a partial inverse agonist with an efficacy of −0.31. This shows again that the steady-state GTPase assay is capable of detecting small effects, which may be masked in reporter gene assays.

DISCUSSION

High Constitutive Activity and Na^+Insensitivity of the R State of the hH_4R. The most prominent feature of the hH_4R is its extraordinarily high constitutive activity, which is also reported from mammalian cell systems (*4, 5, 10*) and therefore unlikely to be an artifact of the Sf9 cell system. Surprisingly, in contrast to most other GPCRs, even at Na^+ concentrations of up to 100 mM the constitutive activity of the hH_4R was not eliminated. For comparison, constitutive activity of receptors like FPR-26 (*41*), complement 5a-receptor (*41*), α_{2B}- and α_{2D}-adrenoceptor (*42*) is completely eliminated by 100 mM of Na^+. Moreover, Na^+ reduces the binding of agonists at opioid receptors (*45*) or the somatostatin receptor subtype SSTR2 (*46*) by stabilizing the inactive R state of the receptor. Mutational experiments with the α_{2a}-adrenoceptor suggested that a highly conserved aspartate in transmembrane domain 2 (TM2) is responsible for the allosteric effects of Na^+ (*47*). When this negatively charged amino acid was replaced by an uncharged amino acid (D79N and D79Q), the effect of Na^+ was eliminated and the mutants were insensitive to the guanine nucleotide 5′-guanylylimidodiphosphate (Gpp(NH)p) in high-affinity agonist binding (*47*).

Surprisingly, the hH_4R also showed GTPγS-insensitive high-affinity agonist binding and Na^+ insensitivity, despite the presence of the highly conserved aspartate in TM2 (D61). Maybe, compared to other GPCRs, D61 in the hH_4R shows a different spatial arrangement in its amino acid environment, or the stabilizing effect of Na^+ on the R state of GPCRs could be mediated by a completely different and as yet unidentified binding site. The Na^+ insensitivity of the R state of the hH_4R is in good agreement with its G-protein-independent high-affinity state. Provided that the high-affinity state and the active-state R* have identical conformations, these findings indicate that the R/R* equilibrium of the hH_4R is extremely shifted to the side of the R* state.

Efficacy of $hH_4R/G\alpha_{i2}$ Interaction. Surprisingly, despite its high constitutive activity, the hH_4R induced only a very slow GDP/GTPγS exchange. It is unlikely that the hH_4R shows a higher selectivity for other G-protein isoforms, since the preference of the hH_4R for $G\alpha_{i2}$ was clearly shown in our experiments (Figure 6). Moreover, coupling of the hH_4R to pertussis-toxin (PTX) sensitive G-proteins was previously demonstrated in mammalian cells like mast cells (*13*) and eosinophils (*18*). The slow G-protein activation kinetics of the hH_4R suggests sustained and prolonged responses to HA under physiological conditions, supporting long-time inflammatory processes. This potentially complements the short-term effects of other faster responding GPCRs, e.g. FPR-26.

THIO is not a Full Inverse Agonist at the hH_4R. Figure 5 shows that NaCl at increasing concentrations still reduces GTPase activity in the presence of 10 μM THIO. Thus, despite of its low potency in the $hH_4R/G\alpha_{i2}$ system, NaCl is more efficient at stabilizing the R state of the hH_4R than THIO, suggesting that THIO is not a full inverse hH_4R agonist. However, in the literature THIO was reported to be a full inverse agonist, since it inhibited the constitutive hH_4R activity in reporter gene assays with hH_4R-transfected SK-N-MC cells to the same extent as treatment with pertussis toxin (*10*).

However, it is very difficult if not impossible to ADP-ribosylate all G_i-proteins by pertussis toxin in intact cells (*40*). Therefore, we determined the true efficacy of thioperamide by comparing the maximum thioperamide effect in the coexpression system ($hH_4R + G\alpha_{i2} + G\beta_1\gamma_2$) with a background membrane expressing only $G\alpha_{i2}$ and $G\beta_1\gamma_2$. The

background membrane defines the effect of a full-inverse agonist. We have shown in [^{35}S]GTPγS binding kinetic experiments that, despite the presence of saturating concentrations of THIO (10 μM), [^{35}S]GTPγS binding to the coexpression membrane was still higher than in the hH_4R-free background membrane. Thus, thioperamide is only a partial inverse agonist at the hH_4R. Similar results were previously reported for the β_2AR expressed in Sf9 cells. Specifically, the inverse β_2AR agonist erythro-DL-1(7-methylindan-4-yloxy)-3-isopropylamino-butano-2-ol (ICI-115881) was not able to completely inhibit the GTP-induced adenylyl cyclase activation (*48*)

In many receptors, the inactive state is stabilized by the ionic lock, an interaction between a highly conserved glutamate in TM6 and the arginine of the DRY motif (TM3). Recently, the crystal structure of the human β_2AR in complex with the inverse agonist carazolol was reported (*49*). In the β_2AR structure, the large distance between R131 of the DRY motif and E268 in TM6 prevents the formation of a tight ionic interaction, resulting in a relatively high constitutive activity of the β_2AR. Even the strong inverse agonist carazolol was not able to completely block the spontaneous receptor activity in GTPγS binding assays. Thus, like THIO at hH_4R, carazolol is only a partial inverse agonist at the β_2AR. Interestingly, in the hH_4R the ionic lock is completely missing, since there is an alanine instead of a glutamate in position 298 (*4*). This may explain the high constitutive activity of the hH_4R, which is even partially resistant to THIO.

A G-Protein-Independent High-Affinity State of the hH_4R. The most interesting and unexpected finding of our study was the GTPγS resistance of the high-affinity state of the hH_4R. In general, guanine nucleotides are expected to reduce affinity and B_{max} values of agonistic radioligands, because the ternary complex model postulates the highest agonist affinity when the receptor is in complex with the agonist and the guanine nucleotide-free G-protein (*21, 36, 38*). The unusual behavior of the hH_4R could be explained by a tight $hH_4R/G\alpha_{i2}$ interaction, which is not disrupted by GTPγS. However, as shown in Table 1, in membranes expressing only the hH_4R without mammalian G-proteins, the [^{3}H]HA high-affinity state was fully conserved. Moreover, the K_i values of JNJ-7777120 and THIO did not change in the absence of mammalian G-proteins, although these ligands are inverse agonists that should prefer the uncoupled R state.

It could be argued that insect cell $G\alpha_i$ (*50*) may interact with the hH_4R in the absence of mammalian G-proteins. However, in steady-state GTPase assays and GTPγS binding studies, G-protein stimulation was hardly detectable in the absence of mammalian G-proteins. This suggests that the hH_4R does not efficiently couple to insect cell $G\alpha_i$-like proteins but can exist in a G-protein-independent high-affinity conformation. This is corroborated by the hH_4R-$G\alpha_{i2}$ fusion protein that shows a coupling factor of ~1 (Table 1), indicating that only the fused G-protein but no insect cell G-proteins are activated.

Guanine-nucleotide insensitivity of high-affinity agonist binding and the existence of a G-protein-independent high-affinity receptor state were also reported for other GPCRs in other cellular systems. A splice variant of the histamine H_3 receptor, $hH_3R(365)$, showed GDP- and GTPγS-insensitive agonist binding (*51*). A high-affinity conformation, which is stable in the absence of G-proteins, was also described for the human dopamine D_3 receptor in CHO cells (*52*). The somatostatin receptor SSTR1 also shows high-affinity agonist binding, which is insensitive to both Na^+ (*46*) and GTPγS (*53*). This indicates that the ternary complex model is not sufficient to describe the G-protein interactions of other GPCRs.

Structural Instability of the hH_4R and the Effect of hH_4R Ligands During Receptor Expression. Both the presence of the agonist HA and the presence of the inverse agonist THIO during receptor expression increased the B_{max} value of the hH_4R in [^{3}H]HA binding (Table 2). The pharmacological properties of the ligands were not important for this effect, suggesting a conformational stabilization of the receptor rather than a conventional up-regulation, which normally is mainly driven by antagonists or inverse agonists. This was confirmed by immunoblots, where the protein expression level was not increased by HA or THIO. A stabilizing effect of ligands was previously reported for the constitutively active mutant of the β_2AR_{CAM} (*29*). The B_{max} in [^{3}H]DHA binding was increased by addition of the agonist isoproterenol or the inverse agonist (ICI-118551) during the receptor expression period. This effect was not observed with the wild-type β_2AR, indicating that the destabilization is caused by the constitutive activity. Similarly, the constitutively active wild-type α_{2A} adrenoceptor (α_{2A}AR) and the α_{2A}AR T373K mutant were stabilized by both agonists and inverse agonists (*30*). Also, the constitutively active human histamine H_2R expressed in CHO cells (*54*) as well as the constitutively active hH_2R mutants D115A and R116A (*55*) showed ligand-aided stabilization. Here, we describe for the first time the same effect for the highly constitutively active wild-type hH_4R.

Ligand-Mediated hH_4R Stabilization in Stability Assays at 37 °C. Stability assays with isolated membranes revealed high instability of the hH_4R and significant stabilization by HA and THIO (Figure 8). Surprisingly, THIO was even able to refold misfolded [^{3}H]HA binding sites. Apparently, at 37 °C the HA binding region of the hH_4R undergoes a conformational change, which prevents access and binding of [^{3}H]HA. However, the ability of THIO to "repair" the HA binding site indicates that, despite the loss of [^{3}H]HA binding sites, THIO is still able to interact with the receptor.

A similar effect was previously described for the inverse agonist (+)-RX 811059 (2-[2-(2-ethoxy-1,4-benzodioxan-2-yl)-1-imidazoline) at the Thr373Lys α_{2A} adrenoceptor mutant (*30*). After 2 h of incubation at 37 °C in the presence of (+)-RX 811059, the amount of [^{3}H]RX 821002 ([^{3}H] (1,4-[6,7(n)-[^{3}H]-benzodioxan-2-methoxy-2-yl)-2-imidazoline) binding sites exceeded the control values. However, this effect was not investigated in more detail (*30*). The highly constitutively active β_2AR_{CAM} mutant behaved similarly in stability assays at 37 °C (quantification of [^{3}H]DHA binding B_{max}) (*29*). The inverse agonist ICI-118551 and the agonist isoproterenol stabilized β_2AR_{CAM}. ICI-118551 was slightly more effective than isoproterenol, but the amount of inverse agonist stabilized [^{3}H]DHA binding sites did not exceed the control values.

It may be a common mechanism that inverse agonists refold denaturated receptors, leading to upregulation of binding sites without increasing the number of receptor molecules in the membrane. When entering the cytoplasm,

however, such ligands may also act as pharmacological chaperones, which assist receptor folding in the endoplasmic reticulum (*56*).

Physiological Relevance of the High Constitutive Activity of the hH$_4$R. Due to the Na^+ insensitivity of the R state, the constitutive activity of the hH_4R may be retained under physiological conditions in the presence of Na^+ concentrations from 15 mM (intracellular) to 145 mM (extracellular). Maybe, the constitutive activity of the hH_4R maintains a certain basal G-protein activation level in immune cells. The slow G-protein activation kinetics of the hH_4R suggests a long-term function such as priming of immune cells, rather than induction of short-term chemotactic effects. In fact, stimulation of the hH_4R by HA enhanced both the chemotactic activity of eotaxin on eosinophils (*18*) and of CXCL-12 on mast cell precursors (*57*).

An important question is how the constitutive activity of the hH_4R may be regulated. Glycosylation of the hH_4R is important for the cell surface expression of intact receptors, similar to what was previously described for FPR-26 (*28*). The expression level and potentially the constitutive activity of the hH_4R may be regulated by changes in glycosylation pattern. Potential scaffolding proteins that modify the interaction between the hH_4R and $G\alpha_{i2}$ could also regulate constitutive activity. The structural instability of the hH_4R provides another regulatory mechanism. In inflamed tissue, the temperature is elevated, possibly causing denaturation of the hH_4R. However, HA released in the area of inflammation may stabilize the H_4R, which then mediates chemotaxis or primes immune cells.

The instability of the H_4R may have implications for drugs that target GPCRs. Inverse agonists cause "functional upregulation" of the receptor by increasing the number of correctly folded receptor molecules. This may cause rebound effects when treatment is discontinued, since the endogenous agonist then activates an increased number of conformationally intact receptors.

It has been reported that constitutive receptor activity is the cause of several diseases (*20*). An enhanced spontaneous activity of the hH_4R may cause chronic pruritus or inflammatory diseases. For these diseases, inverse agonists should be more effective than neutral hH_4R antagonists.

In conclusion, the hH_4R shows an extraordinarily high constitutive activity, which, in contrast to other chemoattractant receptors, is highly resistant to Na^+. Special properties like the guanine-nucleotide-insensitive high-affinity state, which is also preserved in the absence of G_i-proteins, the high conformational instability, and the stabilizing effect of HA and THIO give the hH_4R an exceptional position among the known histamine receptors.

ACKNOWLEDGMENT

We would like to thank Mrs. Gertraud Wilberg, Mrs. Astrid Seefeld, and Mr. Christian Neuhofer for their excellent technical assistance. Thanks are also due to the reviewers for their helpful critique.

REFERENCES

1. Hill, S. J., Ganellin, C. R., Timmerman, H., Schwartz, J. C., Shankley, N. P., Young, J. M., Schunack, W., Levi, R., and Haas, H. L. (1997) International Union of Pharmacology. XIII. Classification of histamine receptors. *Pharmacol. Rev. 49*, 253–278.
2. Raible, D. G., Lenahan, T., Fayvilevich, Y., Kosinski, R., and Schulman, E. S. (1994) Pharmacologic characterization of a novel histamine receptor on human eosinophils. *Am. J. Respir. Crit. Care Med. 149*, 1506–1511.
3. Zhu, Y., Michalovich, D., Wu, H., Tan, K. B., Dytko, G. M., Mannan, I. J., Boyce, R., Alston, J., Tierney, L. A., Li, X., Herrity, N. C., Vawter, L., Sarau, H. M., Ames, R. S., Davenport, C. M., Hieble, J. P., Wilson, S., Bergsma, D. J., and Fitzgerald, L. R. (2001) Cloning, expression, and pharmacological characterization of a novel human histamine receptor. *Mol. Pharmacol. 59*, 434–441.
4. Morse, K. L., Behan, J., Laz, T. M., West, R. E., Jr., Greenfeder, S. A., Anthes, J. C., Umland, S., Wan, Y., Hipkin, R. W., Gonsiorek, W., Shin, N., Gustafson, E. L., Qiao, X., Wang, S., Hedrick, J. A., Greene, J., Bayne, M., and Monsma, F. J., Jr. (2001) Cloning and characterization of a novel human histamine receptor. *J. Pharmacol. Exp. Ther. 296*, 1058–1066.
5. Liu, C., Ma, X., Jiang, X., Wilson, S. J., Hofstra, C. L., Blevitt, J., Pyati, J., Li, X., Chai, W., Carruthers, N., and Lovenberg, T. W. (2001) Cloning and pharmacological characterization of a fourth histamine receptor (H_4) expressed in bone marrow. *Mol. Pharmacol. 59*, 420–426.
6. Nguyen, T., Shapiro, D. A., George, S. R., Setola, V., Lee, D. K., Cheng, R., Rauser, L., Lee, S. P., Lynch, K. R., Roth, B. L., and O'Dowd, B. F. (2001) Discovery of a novel member of the histamine receptor family. *Mol. Pharmacol. 59*, 427–433.
7. Oda, T., Morikawa, N., Saito, Y., Masuho, Y., and Matsumoto, S. (2000) Molecular cloning and characterization of a novel type of histamine receptor preferentially expressed in leukocytes. *J. Biol. Chem. 275*, 36781–36786.
8. Nakamura, T., Itadani, H., Hidaka, Y., Ohta, M., and Tanaka, K. (2000) Molecular cloning and characterization of a new human histamine receptor, HH_4R. *Biochem. Biophys. Res. Commun. 279*, 615–620.
9. Hashimoto, T., Harusawa, S., Araki, L., Zuiderveld, O. P., Smit, M. J., Imazu, T., Takashima, S., Yamamoto, Y., Sakamoto, Y., Kurihara, T., Leurs, R., Bakker, R. A., and Yamatodani, A. (2003) A selective human H_4-receptor agonist: (-)-2-cyano-1-methyl-3-[(2R,5R)-5- [1H-imidazol-4(5)-yl]tetrahydrofuran-2-y] methylguanidine. *J. Med. Chem. 46*, 3162–3165.
10. Lim, H. D., van Rijn, R. M., Ling, P., Bakker, R. A., Thurmond, R. L., and Leurs, R. (2005) Evaluation of histamine H_1-, H_2-, and H_3-receptor ligands at the human histamine H_4 receptor: identification of 4-methylhistamine as the first potent and selective H_4 receptor agonist. *J. Pharmacol. Exp. Ther. 314*, 1310–1321.
11. Thurmond, R. L., Desai, P. J., Dunford, P. J., Fung-Leung, W. P., Hofstra, C. L., Jiang, W., Nguyen, S., Riley, J. P., Sun, S., Williams, K. N., Edwards, J. P., and Karlsson, L. (2004) A potent and selective histamine H_4 receptor antagonist with anti-inflammatory properties. *J. Pharmacol. Exp. Ther. 309*, 404–413.
12. O'Reilly, M., Alpert, R., Jenkinson, S., Gladue, R. P., Foo, S., Trim, S., Peter, B., Trevethick, M., and Fidock, M. (2002) Identification of a histamine H_4 receptor on human eosinophils--role in eosinophil chemotaxis. *J. Recept. Signal Transduction 22*, 431–448.
13. Hofstra, C. L., Desai, P. J., Thurmond, R. L., and Fung-Leung, W. P. (2003) Histamine H_4 receptor mediates chemotaxis and calcium mobilization of mast cells. *J. Pharmacol. Exp. Ther. 305*, 1212–1221.
14. Gutzmer, R., Diestel, C., Mommert, S., Kother, B., Stark, H., Wittmann, M., and Werfel, T. (2005) Histamine H_4 receptor stimulation suppresses IL-12p70 production and mediates chemotaxis in human monocyte-derived dendritic cells. *J. Immunol. 174*, 5224–5232.
15. Dunford, P. J., Williams, K. N., Desai, P. J., Karlsson, L., McQueen, D., and Thurmond, R. L. (2007) Histamine H_4 receptor antagonists are superior to traditional antihistamines in the attenuation of experimental pruritus. *J. Allergy. Clin. Immunol. 119*, 176–183.
16. Varga, C., Horvath, K., Berko, A., Thurmond, R. L., Dunford, P. J., and Whittle, B. J. (2005) Inhibitory effects of histamine H_4 receptor antagonists on experimental colitis in the rat. *Eur. J. Pharmacol. 522*, 130–138.
17. Dunford, P. J., O'Donnell, N., Riley, J. P., Williams, K. N., Karlsson, L., and Thurmond, R. L. (2006) The histamine H_4 receptor mediates allergic airway inflammation by regulating the activation of $CD4^+$ T cells. *J. Immunol. 176*, 7062–7070.

18. Buckland, K. F., Williams, T. J., and Conroy, D. M. (2003) Histamine induces cytoskeletal changes in human eosinophils via the H_4 receptor. *Br. J. Pharmacol. 140*, 1117–1127.
19. Leff, P. (1995) The two-state model of receptor activation. *Trends Pharmacol. Sci. 16*, 89–97.
20. Seifert, R., and Wenzel-Seifert, K. (2002) Constitutive activity of G-protein-coupled receptors: cause of disease and common property of wild-type receptors. *Naunyn−Schmiedeberg's Arch. Pharmacol. 366*, 381–416.
21. Wenzel-Seifert, K., Hurt, C. M., and Seifert, R. (1998) High constitutive activity of the human formyl peptide receptor. *J. Biol. Chem. 273*, 24181–24189.
22. Wenzel-Seifert, K., Arthur, J. M., Liu, H. Y., and Seifert, R. (1999) Quantitative analysis of formyl peptide receptor coupling to $G_i\alpha_1$, $G_i\alpha_2$, and $G_i\alpha_3$. *J. Biol. Chem. 274*, 33259–33266.
23. Houston, C., Wenzel-Seifert, K., Bürckstümmer, T., and Seifert, R. (2002) The human histamine H_2-receptor couples more efficiently to Sf9 insect cell G_s-proteins than to insect cell G_q-proteins: limitations of Sf9 cells for the analysis of receptor/G_q-protein coupling. *J. Neurochem. 80*, 678–696.
24. Kent, R. S., De Lean, A., and Lefkowitz, R. J. (1980) A quantitative analysis of *beta*-adrenergic receptor interactions: resolution of high and low affinity states of the receptor by computer modeling of ligand binding data. *Mol. Pharmacol. 17*, 14–23.
25. Walseth, T. F., and Johnson, R. A. (1979) The enzymatic preparation of [$\alpha-^{32}$P]nucleoside triphosphates, cyclic [^{32}P] AMP, and cyclic [^{32}P] GMP. *Biochim. Biophys. Acta 562*, 11–31.
26. Preuss, H., Ghorai, P., Kraus, A., Dove, S., Buschauer, A., and Seifert, R. (2007) Constitutive activity and ligand selectivity of human, guinea pig, rat, and canine histamine H_2 receptors. *J. Pharmacol. Exp. Ther. 321*, 983–995.
27. Gether, U., Lin, S., and Kobilka, B. K. (1995) Fluorescent labeling of purified β_2 adrenergic receptor. Evidence for ligand-specific conformational changes. *J. Biol. Chem. 270*, 28268–28275.
28. Wenzel-Seifert, K., and Seifert, R. (2003) Critical role of N-terminal N-glycosylation for proper folding of the human formyl peptide receptor. *Biochem. Biophys. Res. Commun. 301*, 693–698.
29. Gether, U., Ballesteros, J. A., Seifert, R., Sanders-Bush, E., Weinstein, H., and Kobilka, B. K. (1997) Structural instability of a constitutively active G protein-coupled receptor. Agonist-independent activation due to conformational flexibility. *J. Biol. Chem. 272*, 2587–2590.
30. Pauwels, P. J., and Tardif, S. (2002) Enhanced stability of wild-type and constitutively active a_{2A}-adrenoceptors by ligands with agonist, silent and inverse agonist properties. *Naunyn−Schmiedeberg's Arch. Pharmacol. 366*, 134–141.
31. Seifert, R., Wenzel-Seifert, K., and Kobilka, B. K. (1999) GPCR-Gα fusion proteins: molecular analysis of receptor-G-protein coupling. *Trends Pharmacol. Sci. 20*, 383–389.
32. Seifert, R., Wenzel-Seifert, K., Bürckstümmer, T., Pertz, H. H., Schunack, W., Dove, S., Buschauer, A., and Elz, S. (2003) Multiple differences in agonist and antagonist pharmacology between human and guinea pig histamine H_1-receptor. *J. Pharmacol. Exp. Ther. 305*, 1104–1115.
33. van Rijn, R. M., Chazot, P. L., Shenton, F. C., Sansuk, K., Bakker, R. A., and Leurs, R. (2006) Oligomerization of recombinant and endogenously expressed human histamine H_4 receptors. *Mol. Pharmacol. 70*, 604–615.
34. Gilman, A. G. (1987) G proteins: transducers of receptor-generated signals. *Annu. Rev. Biochem. 56*, 615–649.
35. De Lean, A., Stadel, J. M., and Lefkowitz, R. J. (1980) A ternary complex model explains the agonist-specific binding properties of the adenylate cyclase-coupled β-adrenergic receptor. *J. Biol. Chem. 255*, 7108–7117.
36. Seifert, R., Lee, T. W., Lam, V. T., and Kobilka, B. K. (1998) Reconstitution of β_2-adrenoceptor-GTP-binding-protein interaction in Sf9 cells--high coupling efficiency in a β_2-adrenoceptor-$G_s\alpha$ fusion protein. *Eur. J. Biochem. 255*, 369–382.
37. Wenzel-Seifert, K., and Seifert, R. (2003) Functional differences between human formyl peptide receptor isoforms 26, 98, and G6. *Naunyn−Schmiedeberg's Arch. Pharmacol. 367*, 509–515.
38. Wenzel-Seifert, K., and Seifert, R. (2000) Molecular analysis of β_2-adrenoceptor coupling to G_s-, G_i-, and G_q-proteins. *Mol. Pharmacol. 58*, 954–966.
39. Gille, A., Wenzel-Seifert, K., Doughty, M. B., and Seifert, R. (2003) GDP affinity and order state of the catalytic site are critical for function of xanthine nucleotide-selective $G\alpha_s$ proteins. *J. Biol. Chem. 278*, 7822–7828.
40. Wenzel-Seifert, K., and Seifert, R. (1990) Nucleotide-, chemotactic peptide- and phorbol ester-induced exocytosis in HL-60 leukemic cells. *Immunobiology 181*, 298–316.
41. Seifert, R., and Wenzel-Seifert, K. (2001) Unmasking different constitutive activity of four chemoattractant receptors using Na^+ as universal stabilizer of the inactive (R) state. *Recept. Channels 7*, 357–369.
42. Tian, W. N., and Deth, R. C. (2000) Differences in efficacy and Na^+ sensitivity between α_{2B} and α_{2D} adrenergic receptors: implications for R and R* states. *Pharmacology 61*, 14–21.
43. Kleemann, P., Papa, D., Vigil-Cruz, S., and Seifert, R. (2008) Functional reconstitution of the human chemokine receptor CXCR4 with G(i)/G (o)-proteins in Sf9 insect cells. *Naunyn−Schmiedeberg's Arch. Pharmacol. 378*, 261–274.
44. Robben, J. H., Sze, M., Knoers, N. V., and Deen, P. M. (2007) Functional rescue of vasopressin V2 receptor mutants in MDCK cells by pharmacochaperones: relevance to therapy of nephrogenic diabetes insipidus. *Am. J. Physiol. Renal Physiol. 292*, F253−260.
45. Pert, C. B., and Snyder, S. H. (1974) Opiate Receptor Binding of Agonists and Antagonists Affected Differentially by Sodium. *Mol. Pharmacol. 10*, 868–879.
46. Kong, H., Raynor, K., Yasuda, K., Bell, G. I., and Reisine, T. (1993) Mutation of an aspartate at residue 89 in somatostatin receptor subtype 2 prevents Na+ regulation of agonist binding but does not alter receptor-G protein association. *Mol. Pharmacol. 44*, 380–384.
47. Ceresa, B. P., and Limbird, L. E. (1994) Mutation of an aspartate residue highly conserved among G-protein-coupled receptors results in nonreciprocal disruption of α_2-adrenergic receptor-G-protein interactions. A negative charge at amino acid residue 79 forecasts α_{2A}-adrenergic receptor sensitivity to allosteric modulation by monovalent cations and fully effective receptor/G-protein coupling. *J. Biol. Chem. 269*, 29557–29564.
48. Seifert, R., Gether, U., Wenzel-Seifert, K., and Kobilka, B. K. (1999) Effects of guanine, inosine, and xanthine nucleotides on β_2-adrenergic receptor/G(s) interactions: evidence for multiple receptor conformations. *Mol. Pharmacol. 56*, 348–358.
49. Rasmussen, S. G. F., Choi, H.-J., Rosenbaum, D. M., Kobilka, T. S., Thian, F. S., Edwards, P. C., Burghammer, M., Ratnala, V. R. P., Sanishvili, R., Fischetti, R. F., Schertler, G. F. X., Weis, W. I., and Kobilka, B. K. (2007) Crystal structure of the human β_2 adrenergic G-protein-coupled receptor. *Nature 450*, 383–387.
50. Knight, P. J., and Grigliatti, T. A. (2004) Diversity of G proteins in Lepidopteran cell lines: partial sequences of six G protein alpha subunits. *Arch. Insect Biochem. Physiol. 57*, 142–150.
51. Bongers, G., Krueger, K. M., Miller, T. R., Baranowski, J. L., Estvander, B. R., Witte, D. G., Strakhova, M. I., van Meer, P., Bakker, R. A., Cowart, M. D., Hancock, A. A., Esbenshade, T. A., and Leurs, R. (2007) An 80-amino acid deletion in the third intracellular loop of a naturally occurring human histamine H_3 isoform confers pharmacological differences and constitutive activity. *J. Pharmacol. Exp. Ther. 323*, 888–898.
52. Vanhauwe, J. F. M., Fraeyman, N., Francken, B. J. B., Luyten, W. H. M. L., and Leysen, J. E. (1999) Comparison of the Ligand Binding and Signaling Properties of Human Dopamine D_2 and D_3 Receptors in Chinese Hamster Ovary Cells. *J. Pharmacol. Exp. Ther. 290*, 908–916.
53. Rens-Domiano, S., Law, S. F., Yamada, Y., Seino, S., Bell, G. I., and Reisine, T. (1992) Pharmacological properties of two cloned somatostatin receptors. *Mol. Pharmacol. 42*, 28–34.
54. Alewijnse, A. E., Smit, M. J., Hoffmann, M., Verzijl, D., Timmerman, H., and Leurs, R. (1998) Constitutive activity and structural instability of the wild-type human H_2 receptor. *J. Neurochem. 71*, 799–807.
55. Alewijnse, A. E., Timmerman, H., Jacobs, E. H., Smit, M. J., Roovers, E., Cotecchia, S., and Leurs, R. (2000) The effect of mutations in the DRY motif on the constitutive activity and structural instability of the histamine H_2 receptor. *Mol. Pharmacol. 57*, 890–898.
56. Bernier, V., Bichet, D. G., and Bouvier, M. (2004) Pharmacological chaperone action on G-protein-coupled receptors. *Curr. Opin. Pharmacol. 4*, 528–533.
57. Godot, V., Arock, M., Garcia, G., Capel, F., Flys, C., Dy, M., Emilie, D., and Humbert, M. (2007) H_4 histamine receptor mediates optimal migration of mast cell precursors to CXCL12. *J. Allergy Clin. Immunol. 120*, 827–834.

BI802050D